

Remodelling in statistically oriented fibre-reinforced materials and biological tissues

*Original*

Remodelling in statistically oriented fibre-reinforced materials and biological tissues / Grillo, Alfio; Wittum, Gabriel; Tomic, Aleksandar; Federico, Salvatore. - In: MATHEMATICS AND MECHANICS OF SOLIDS. - ISSN 1081-2865. - ELETTRONICO. - 20:9(2015), pp. 1107-1129. [10.1177/1081286513515265]

*Availability:*

This version is available at: 11583/2520901 since: 2020-06-01T16:59:10Z

*Publisher:*

SAGE

*Published*

DOI:10.1177/1081286513515265

*Terms of use:*

This article is made available under terms and conditions as specified in the corresponding bibliographic description in the repository

*Publisher copyright*

Sage postprint/Author's Accepted Manuscript

Grillo, Alfio; Wittum, Gabriel; Tomic, Aleksandar; Federico, Salvatore, Remodelling in statistically oriented fibre-reinforced materials and biological tissues, accepted for publication in MATHEMATICS AND MECHANICS OF SOLIDS (20 9) pp. 1107-1129. © 2015 (Copyright Holder). DOI:10.1177/1081286513515265

(Article begins on next page)

1

# Remodelling in Statistically Oriented

2

## Fibre-Reinforced Materials and Biological Tissues\*

3

Alfio Grillo<sup>†</sup>, Gabriel Wittum<sup>‡</sup>, Aleksandar Tomic<sup>§</sup>, Salvatore Federico<sup>¶</sup>

4

### Abstract

5

6

7

8

9

10

11

12

13

14

15

16

We present a mathematical model of structural reorganisation in a fibre-reinforced composite material in which the fibres are oriented statistically, i.e., obey a probability distribution of orientation. Such a composite material exemplifies a biological tissue (e.g., articular cartilage or a blood vessel) whose soft matrix is reinforced by collagen fibres. The structural reorganisation of the composite takes place as fibres reorient, in response to mechanical stimuli, in order to optimise the stress distribution in the tissue. Our mathematical model is based on the Principle of Virtual Powers and the study of dissipation. Besides incompressibility, our main hypothesis is that the composite is characterised by a probability density distribution that measures the probability of finding a family of fibres aligned along a given direction at a fixed material point. Under this assumption, we describe the reorientation of fibres as the evolution of the most probable direction along which the fibres are aligned. To test our theory, we compare our simulations of a benchmark problem with selected results taken from the literature.

17

**Keywords:** Remodelling, Two-layer dynamics, Dissipation, Statistical composites.

---

*\*Dedicated to Prof. Antonio Di Carlo in recognition of his academic activity.*

<sup>†</sup>Corresponding Author. DISMA “G. L. Lagrange”, Politecnico di Torino, Corso Duca degli Abruzzi 24, I-10129, Torino (TO), Italy. Tel.: +39 011 090 7531. Fax: +39 011 090 7599. E-mail: [alfio.grillo@polito.it](mailto:alfio.grillo@polito.it)

<sup>‡</sup>G-CSC, Goethe Universität Frankfurt. Kettenhofweg 139, D-60325, Frankfurt am Main, Germany. E-mail: [gabriel.wittum@gcsc.uni-frankfurt.de](mailto:gabriel.wittum@gcsc.uni-frankfurt.de)

<sup>§</sup>Graduate Programme in Mechanical Engineering, The University of Calgary, 2500 University Drive NW, Calgary, Alberta, T2N1N4, Canada. E-mail: [acotomic@gmail.com](mailto:acotomic@gmail.com)

<sup>¶</sup>Dept. of Mechanical and Manufacturing Engineering, The University of Calgary, 2500 University Drive NW, Calgary, Alberta, T2N1N4, Canada. Tel.: +1 403 220 5790. Fax: +1 403 282 8406. E-mail: [salvatore.federico@ucalgary.ca](mailto:salvatore.federico@ucalgary.ca)

# 1 Introduction

One of the properties of biological tissues is the capability of adapting their internal structure in response to the interactions with the environment in which they are placed. In Biomechanics, the evolution of the internal structure of a tissue is sometimes referred to as “remodelling” [26, 60].

We consider a purely mechanical framework, and focus on tissues that can be modelled as fibre-reinforced composite materials with fibres oriented according to a given probability distribution. Examples of tissues of this type are arteries and articular cartilage. Our approximation of these tissues is quite simplified in this work, since we regard them as solid bodies comprising two constituents only: a soft matrix and collagen fibres. The structure of real tissues is much more complicated than that addressed in our work.

The arterial wall comprehends several fibre-reinforced layers, in each of which the fibres are oriented according to rather well defined patterns [35]. Three main strata can be detected. These are referred to as *intima*, *media*, and *adventia*, and represent, respectively, the inner, the middle, and the outer stratum of an artery. The *intima* is the thinnest stratum. It comprises a single layer of endothelial cells located on a basal membrane. The *media* consists of muscle cells and collagen fibrils. It features several fibre-reinforced layers, in each of which the fibres are coiled helically. The direction of the helix in a layer is opposite to that in the consecutive one. Finally, the *adventia* consists of thick bundles of collagen fibres, arranged helically, which have the task of reinforcing the outermost stratum of the arterial wall. More details about the mechanics of arterial walls can be found in the papers by Holzapfel et al. [35] and Gasser et al. [29].

Articular cartilage is a multiphasic, multi-species material. The species can be identified with solid particles, fluids, chemicals and, in particular, ions [42]. The overall mechanical behaviour of the solid phase of articular cartilage is influenced by the presence of inclusions. These are identified with chondrocytes (i.e., the cells that synthesise extra-cellular matrix) and collagen fibres [see, e.g., 49, and references therein]. The latter ones contribute to the tissue overall capability of bearing loads, and are arranged in a way that adapts to the mechanical loading. Given a sample of articular cartilage, three zones can be identified, based on histological features (chondrocyte shape and collagen fibre orientation): the deep zone, which is proximal to the tidemark (bone-cartilage

46 interface), the middle zone, and the superficial zone, which is close to the articular surface. A  
 47 property of articular cartilage is that the arrangement of collagen fibres depends on the location  
 48 at which the fibres are placed inside the tissue. The fibres are nearly parallel to the tissue depth  
 49 in the deep zone, randomly oriented in the middle zone, and parallel to the articular surface in  
 50 the superficial zone [2, 48]. A linear elastic model of articular cartilage based on a statistical  
 51 orientation of collagen fibres was proposed by Federico et al. [23], where the tissue was studied as a  
 52 transversely isotropic, transversely homogenous, multiphasic composite material. The theoretical  
 53 tools were developed by in a previous work [22] on the basis of Walpole's algebra of fourth-order  
 54 tensors [63].

55 Under the action of mechanical stimuli, the body deforms and the fibres reorient. While the  
 56 first process is the standard change of shape of a body subjected to applied loads, prescribed  
 57 displacements, or combination of both, the second process triggers a reorganisation of the internal  
 58 structure of the body and, in this sense, represents a type of remodelling.

59 In many cases of interest, the reorientation of the collagen fibres should be investigated in  
 60 conjunction with the secretion and removal of the fibres themselves. Grillo et al. [31] presented  
 61 a more comprehensive framework in which growth, interphase mass transfer, and remodelling in  
 62 fibre-reinforced, multi-constituent materials were studied. This model remained, however, at the  
 63 theoretical level, since the solution of the determined equations requires a detailed mathematical  
 64 analysis and is, for this reason, still work in progress. Hence, in order to test the theory presented  
 65 in the present work by handling quite manageable numerical examples, we focussed here on some  
 66 aspects of remodelling that are conceptually independent on growth.

67 One reason for studying remodelling is to determine how the effective quantities characterising a  
 68 tissue evolve in time. Examples of such quantities are the mechanical stiffness and the permeability  
 69 of the tissue, cf. e.g., [19, 20, 21].

70 In the case of hyperelastic materials undergoing large deformations, the presence of fibres is  
 71 accounted for by introducing the structure tensor in the list of arguments of the body strain energy  
 72 function. For example, this approach was adopted by Holzapfel et al. [35] and Menzel [46, 47] for  
 73 arterial walls. The structure tensor is defined by  $\mathbf{a} := \mathbf{m} \otimes \mathbf{m}$ , where  $\mathbf{m}$  is a unit vector describing

the local alignment of a fibre along a prescribed direction of space. If  $\mathbf{m}$  follows the deformation of the body, its evolution is determined by  $\mathcal{L}_v \mathbf{m} = -\mathbf{d}_m \mathbf{m}$  [9], where  $\mathcal{L}_v$  is the Lie-derivative operator,  $\mathbf{v}$  is the velocity,  $\mathbf{d}_m := \mathbf{m}(\mathbf{d}\mathbf{m})$ , and  $\mathbf{d}$  is the symmetric part of the velocity gradient. This identity, being purely kinematic, contains neither phenomenological parameters nor material properties.

Imatani and Maugin [37] developed a mathematical model of growth and reorientation of fibres in anisotropic hyperelastic media in which the Kröner-Lee decomposition of the deformation gradient tensor [5, 38, 40, 56], and the concept of reference crystal [16] were used to modify  $\mathcal{L}_v \mathbf{m} = -\mathbf{d}_m \mathbf{m}$ .

Driessen et al. [15] studied changes in the content and orientation of collagen fibres in soft connective tissues due to mechanical interactions, and related the configuration of the fibres to the macroscopic stress in the tissue. Ohsumi et al. [52] performed simulations of anisotropic collagen gel compaction.

Recently, studies on the biomechanical behaviour of biological tissues reinforced by collagen fibres, such as the abdominal aorta, have been performed, e.g., by deBotton and Shmuel [13], Schriebl et al. [58], and Gasser et al. [28]. A review on the subject was written by [62]. In studying the reorientation of fibres in arteries, Olsson and Klarbring [53] proposed a model in which the angles defining the local fibre orientation were treated as additional degrees of freedom of the body, rather than as internal variables, and were determined by solving specific balance laws. A comparison of the results of Olsson and Klarbring [53] with those of Imatani and Maugin [37] was done by Grillo et al. [32].

In this work, we propose a model that aims to extend the treatment of remodelling given by Olsson and Klarbring [53] to the case of a composite material featuring a statistical distribution of reinforcing fibres. We assume that the composite material is transversely isotropic with respect to a given symmetry axis, and that the fibres are oriented according to a Gaussian probability density distribution. We denote by  $Q$  the angle around which the Gaussian distribution is peaked, and refer to it as to the “remodelling variable”. We treat  $Q$  as an additional kinematic descriptor. The implications of this choice and the differences between the work of Olsson and Klarbring [53]

and ours are discussed in sections 4 and 8. Other authors who have used the concept of probability density distribution for modelling fibre-reinforced composite materials are, e.g., [4], and [39].

The remainder of this work is organised as follows. In section 2 we introduce the notation. In section 3, we discuss the composite materials with statistical orientation of fibres. In section 4, we present the Principle of Virtual Powers. In section 5, we study the dissipation and develop the constitutive theory. In section 6, we present in detail a demonstration problem. Results are presented in section 7 and summarised in section 8.

## 2 General Notation

For the sake of generality, the covariant formalism is adopted throughout this paper and the notation introduced by Truesdell and Noll [61] and Marsden and Hughes [45], with slight modifications, is employed.

Let  $\mathcal{B}$  and  $\mathcal{E}$  be a body and the three-dimensional Euclidean space, respectively. The reference configuration of the body is denoted by  $\mathcal{C} \subset \mathcal{E}$ . The set  $[t_0, t_f) \subset \mathbb{R}$  is the interval of time over which the evolution of the body is observed. The motion of the body is described by the smooth function  $\chi : \mathcal{C} \times [t_0, t_f) \rightarrow \mathcal{E}$ . The set  $\mathcal{C}_t = \chi(\mathcal{C}, t) \subset \mathcal{E}$  is the region of space occupied by the body at time  $t$ . It holds that  $\chi(X, t) = x$ , with  $x \in \mathcal{E}$  and  $X \in \mathcal{C}$ .

The spaces  $T_x\mathcal{E}$  and  $T_X\mathcal{C}$  are said to be the tangent spaces attached, respectively, to  $\mathcal{E}$  and  $\mathcal{C}$  at the points  $x$  and  $X$ . Their dual spaces,  $T_x^*\mathcal{E}$  and  $T_X^*\mathcal{C}$ , are referred to as cotangent spaces. The tangent and cotangent bundles associated with  $\mathcal{C}$  are defined by  $T\mathcal{C} := \bigcup_{X \in \mathcal{C}} T_X\mathcal{C}$  and  $T^*\mathcal{C} := \bigcup_{X \in \mathcal{C}} T_X^*\mathcal{C}$ , respectively. The tangent and cotangent bundles associated with  $\mathcal{E}$ ,  $T\mathcal{E}$  and  $T^*\mathcal{E}$ , are defined in a similar fashion.

Let  $\mathcal{A}$  be a linear vector space, and let  $\mathcal{A}^*$  be its dual space. Then,  $\mathcal{A} \otimes \mathcal{A}$  denotes the space of all real-valued, second-order tensors  $\mathbf{a} : \mathcal{A}^* \times \mathcal{A}^* \rightarrow \mathbb{R}$ , whereas  $(\mathcal{A} \otimes \mathcal{A})_S$  is the subspace of all symmetric second-order tensors belonging to  $\mathcal{A} \otimes \mathcal{A}$ . Moreover, given two linear spaces  $\mathcal{A}$  and  $\mathcal{Z}$ ,  $\mathcal{A} \otimes \mathcal{Z}^*$  represents the space of all two-point tensors  $\mathbf{f} : \mathcal{A}^* \times \mathcal{Z} \rightarrow \mathbb{R}$ .

The spaces  $T\mathcal{E}$  and  $T\mathcal{C}$  are assumed to be equipped with the metric tensors  $\mathbf{g} \in T^*\mathcal{E} \otimes T^*\mathcal{E}$

128 and  $\mathbf{G} \in T^*\mathcal{C} \otimes T^*\mathcal{C}$ , respectively. For all pairs  $(\mathbf{u}, \mathbf{v}) \in T_x\mathcal{E} \times T_x\mathcal{E}$  and  $(\mathbf{U}, \mathbf{V}) \in T_X\mathcal{C} \times T_X\mathcal{C}$ , the  
 129 scalar products  $\mathbf{u} \cdot \mathbf{v}$  and  $\mathbf{U} \cdot \mathbf{V}$  are defined by  $\mathbf{u} \cdot \mathbf{v} = u^a g_{ab}(x) v^b$  and  $\mathbf{U} \cdot \mathbf{V} = U^A G_{AB}(X) V^B$ .

130 The identities in  $T\mathcal{E}$  and  $T\mathcal{C}$  are denoted by  $\mathbf{i} \in T\mathcal{E} \otimes T^*\mathcal{E}$  and  $\mathbf{I} \in T\mathcal{C} \otimes T^*\mathcal{C}$ , respectively. It  
 131 holds that  $\mathbf{i} = \mathbf{g}^{-1}\mathbf{g}$  and  $\mathbf{I} = \mathbf{G}^{-1}\mathbf{G}$ .

132 The two-point tensor  $\mathbf{F} \in T\mathcal{E} \otimes T^*\mathcal{C}$ , with components  $F^a_A = \partial\chi^a/\partial X^A$  and determinant  
 133  $J = \det(\mathbf{F}) > 0$ , is the deformation gradient tensor. The Cauchy-Green deformation tensor is  
 134 defined as  $\mathbf{C} = \mathbf{F}^T \mathbf{g} \mathbf{F} = \mathbf{F}^T \cdot \mathbf{F} \in T^*\mathcal{C} \otimes T^*\mathcal{C}$ , with  $\mathbf{F}^T \in T^*\mathcal{C} \otimes T\mathcal{E}$ . The inverse of  $\mathbf{C}$  is denoted by  
 135  $\mathbf{B} := \mathbf{C}^{-1} \in T\mathcal{C} \otimes T\mathcal{C}$ .

136 The deformation gradient tensor  $\mathbf{F}$  can be decomposed into a volumetric and an isochoric  
 137 part [25, 51], that is  $\mathbf{F} = J^{1/3} \bar{\mathbf{F}}$ . The isochoric part,  $\bar{\mathbf{F}}$ , has unitary determinant, i.e.,  $\det(\bar{\mathbf{F}}) =$   
 138 1. Consequently, the Cauchy-Green deformation tensor becomes  $\mathbf{C} = J^{2/3} \bar{\mathbf{C}}$ , with  $\bar{\mathbf{C}} = \bar{\mathbf{F}}^T \cdot \bar{\mathbf{F}}$ .  
 139 Furthermore, let  $\mathbf{\Upsilon}(\mathbf{C}) := [\det(\mathbf{C})]^{-1/3} \mathbf{C} = \bar{\mathbf{C}}$  be an auxiliary function defined for all symmetric,  
 140 non-singular tensors of  $T^*\mathcal{C} \otimes T^*\mathcal{C}$ , and valued in the set of symmetric, unimodular tensors of the  
 141 same type. By definition,  $\mathbf{\Upsilon}$  is homogeneous of degree zero. Its derivative reads

$$\frac{\partial \mathbf{\Upsilon}}{\partial \mathbf{C}}(\mathbf{C}) = [\det(\mathbf{C})]^{-1/3} [\mathbb{M}(\mathbf{C})]^T, \quad \mathbb{M}(\mathbf{C}) = \mathbb{I} - \frac{1}{3} \mathbf{B} \otimes \mathbf{C}. \quad (1)$$

142 The fourth-order tensor  $\mathbb{I}$  is the identity in  $(T\mathcal{C} \otimes T\mathcal{C})_S$  (please, see Appendix).

143 The measures of stress used in this work are the first and the second Piola-Kirchhoff stress  
 144 tensors, i.e.,  $\mathbf{P} \in T\mathcal{E} \otimes T\mathcal{C}$  and  $\mathbf{S} = \mathbf{F}^{-1} \mathbf{P} \in (T\mathcal{C} \otimes T\mathcal{C})_S$ . The tensor

$$\mathbf{S}_d := \mathbb{M}(\mathbf{C}) : \mathbf{S} = \mathbf{S} - \frac{1}{3} \text{tr}[\mathbf{C}\mathbf{S}] \mathbf{B} \quad (2)$$

145 represents the distortional part of  $\mathbf{S}$  and satisfies identically the condition  $\text{tr}[\mathbf{C}\mathbf{S}_d] = 0$ , i.e.,  $\mathbf{S}_d$  is  
 146 deviatoric with respect to the metric induced by  $\mathbf{C}$ . The distortional part of  $\mathbf{P}$  is defined by

$$\mathbf{P}_d := \mathbf{F} \mathbf{S}_d = \mathbf{P} - \frac{1}{3} \text{tr}[\mathbf{g} \mathbf{P} \mathbf{F}^T] \mathbf{g}^{-1} \mathbf{F}^{-T}. \quad (3)$$

147 Finally, by introducing the Cauchy stress tensor  $\boldsymbol{\sigma} = J^{-1} \mathbf{P} \mathbf{F}^T = J^{-1} \mathbf{F} \mathbf{S} \mathbf{F}^T$ , and post-multiplying

148 (3) by  $\mathbf{F}^T$ , the expression of the deviatoric part of Cauchy stress

$$\boldsymbol{\sigma}_d := J^{-1} \mathbf{P}_d \mathbf{F}^T = \boldsymbol{\sigma} - \frac{1}{3} \text{tr}[\mathbf{g}\boldsymbol{\sigma}] \mathbf{g}^{-1} \quad (4)$$

149 is arrived at. The tensor  $\boldsymbol{\sigma}_d$  is deviatoric with respect to the metric generated by  $\mathbf{g}$ .

### 150 3 Composite materials with statistical orientation of fibres

151 The fibre-reinforced composite materials studied in this paper are assumed to comply with the  
 152 following hypotheses: (a) they can be modelled as saturated biphasic mixtures featuring a matrix  
 153 (phase  $m$ ) and several families of fibres (phase  $f$ ), (b) both phases are constrained to move with  
 154 the same macroscopic velocity, and (c) each phase is intrinsically incompressible and exhibits  
 155 hyperelastic material behaviour. Moreover, the fibres are assumed to be oriented in space according  
 156 to a probability density distribution whose functional form is prescribed from the outset on the  
 157 basis of experimental data [2, 48].

158 The knowledge of the internal structure of composite materials of the kind described above  
 159 can be encapsulated into two pieces of information: the volumetric fraction of the fibres and a  
 160 distribution that measures the probability density of finding a family of fibres aligned along a  
 161 chosen direction at a given material point. In general, one has to speak of “a family of fibres”  
 162 rather than of “a fibre”, since fibres with different geometric and/or mechanical properties may be  
 163 aligned along the same spatial direction.

#### 164 3.1 Consequences of the hypotheses (a), (b) and (c)

165 At a sufficiently coarse scale of observation, a composite material of the kind considered in this work  
 166 can be viewed as a mixture of solids [3]. For the purposes of this article, the mixture is assumed to  
 167 comprise only two solid phases, which are characterised by different mechanical properties and are  
 168 separated by an interface. The physical fields that determine the amount of a given phase in the  
 169 mixture are the true, or intrinsic, mass density and the volumetric fraction of the considered phase.  
 170 The true mass densities are denoted by  $\varrho_f$  and  $\varrho_m$ . The volumetric fractions are indicated by  $\varphi_f$



171 and  $\varphi_m$ . The saturation constraint is expressed by  $\varphi_f + \varphi_m = 1$ , which must be satisfied at all  
 172 times and at all points of the mixture. Moreover, the admissible values of each volumetric fraction  
 173 range in the interval  $[0, 1]$ . The mass density of the composite material as a whole is defined by  
 174  $\varrho = \varphi_f \varrho_f + \varphi_m \varrho_m$ . All fields are defined here according to the Eulerian (or spatial) description of  
 175 Continuum Mechanics.

176 Assuming that matrix and fibres move with the same velocity places the restriction that the  
 177 mass balance law of each constituent must comply with the chain of equalities

$$\operatorname{div}(\mathbf{v}) = -\frac{D_t \varphi_f}{\varphi_f} - \frac{D_t \varrho_f}{\varrho_f} = \frac{D_t \varphi_f}{1 - \varphi_f} - \frac{D_t \varrho_m}{\varrho_m}, \quad (5)$$

178 with  $\mathbf{v}$  and  $D_t$  being the velocity and the convective derivative operator, respectively.

179 Requiring each constituent of the mixture to be incompressible means to set the ratios  $D_t \varrho_f / \varrho_f$   
 180 and  $D_t \varrho_m / \varrho_m$  equal to zero in (5). This yields

$$\operatorname{div}(\mathbf{v}) = 0, \quad (6a)$$

$$D_t \varphi_f = 0. \quad (6b)$$

181 Since (6a) implies  $J = 1$ , the Piola transformation of  $\varphi_f$  reads  $\Phi_f := J \phi_f = \phi_f$ , with  $\phi_f(\cdot, t) =$   
 182  $\varphi_f(\cdot, t) \circ \chi(\cdot, t)$ . The quantity  $\Phi_f$  is the volumetric fraction of the “fibres” as measured in the  
 183 reference configuration. It follows from (6a) and (6b) that  $\dot{\Phi}_f = 0$ . The volumetric fractions  $\Phi_f$  and  
 184  $\Phi_m = 1 - \Phi_f$  may generally depend on the point of  $\mathcal{C}$  at which they are evaluated.

185 The condition (6a) can be rephrased as

$$\overline{\ln(J)} = \operatorname{tr}[(\operatorname{Grad} \mathbf{u}) \mathbf{F}^{-1}] = 0, \quad (7)$$

186 with  $\mathbf{u} : \mathcal{C} \times [t_0, t_f) \rightarrow T\mathcal{E}$  being defined by  $\mathbf{u}(\cdot, t) = \mathbf{v}(\cdot, t) \circ \chi(\cdot, t)$ , and  $\operatorname{Grad} \mathbf{u}$  being the  
 187 material velocity gradient. The conditions (6) also imply  $D_t \varrho = 0$ .

### 3.2 Probability density distribution (PDD)

A fibre-reinforced composite material with statistically oriented fibres is generally an anisotropic medium. To model anisotropy for materials of this kind, one has to introduce the set of all directions in space and a probability density distribution (PDD) defined on it. The set of all directions is locally identified with the unit hemisphere  $\mathbb{H}^2 := \{\mathbf{M} \in T_X\mathcal{C} : \|\mathbf{M}\| = 1, \text{ and } \mathbf{M} \cdot \mathbf{\Xi} \geq 0\}$  attached to  $X \in \mathcal{C}$ , where  $\mathbf{\Xi}$  is the local axis of symmetry of transverse isotropy. If  $\{\mathbf{N}_A\}_{A=1}^3 \subset T_X\mathcal{C}$  is an orthonormal vector basis of  $T_X\mathcal{C}$ , and  $\mathbf{N}_3$  is chosen as the polar axis, the unit vector  $\mathbf{M}$  can be expressed in terms of the co-latitude  $\alpha$  from the polar axis and the longitude  $\beta$  from the  $\mathbf{N}_1$ - $\mathbf{N}_2$  plane:

$$\mathbf{M} = \sin(\alpha) \cos(\beta) \mathbf{N}_1 + \sin(\alpha) \sin(\beta) \mathbf{N}_2 + \cos(\alpha) \mathbf{N}_3. \quad (8)$$

The PDD  $\wp$  of finding a fibre locally oriented along the direction  $\mathbf{M}$  is defined on the set  $\mathbb{H}^2$ , and is determined by a set of parameters that describe the internal structure of the composite. Depending on the addressed problem and the modelled material, several choices of  $\wp$  are possible. For example, a Gaussian distribution has been proposed by Federico et al. [22, 23], while  $\pi$ -periodic von Mises distributions have been used by Gasser et al. [29]. Any choice of the PDD has to comply with the following restrictions: (i)  $\wp$  has to fulfill the normalisation condition; (ii) it has to be an even function of  $\mathbf{M}$ ; and (iii) it has to reflect the material symmetries of the composite that it models.

In this work, the composite material is assumed to exhibit transverse isotropy with respect to the axis determined by  $\mathbf{N}_3$ , which is thus taken as symmetry axis for the whole reference configuration  $\mathcal{C}$ . To be consistent with this feature,  $\wp$  cannot depend on the latitude  $\beta$ . Furthermore,  $\wp$  is postulated to be a Gaussian distribution. This requirement implies that  $\wp$  depends on two parameters only, which are the variance,  $\varpi^2$ , and the angle  $Q$  defining the most probable direction of fibres' alignment. In general, both parameters should be regarded as functions of time and position of material particles. Their dependence on  $X$  supplies information about the inhomogeneity with which the fibres are oriented in the composite, whereas their evolution in time accounts for the time-dependent structural adaptation of the composite in response to some remodelling force. In

the following, however,  $\varpi$  shall be regarded as a given constant and assigned from the outset. Although this is a strong assumption for some practical cases, it allows to keep the model at an acceptable level of complexity. On the basis of the considerations above, the PDD is taken as

$$\wp(\mathbf{M}, Q) := \frac{g(\mathbf{M}, Q)}{\int_{\mathbb{H}^2} g(\mathbf{M}', Q) dS'}. \quad (9)$$

If the re-parameterisation (8) is used, the definition (9) can be reformulated as

$$\wp(\alpha, Q) := \frac{g(\alpha, Q)}{\int_0^{2\pi} \left\{ \int_0^{\pi/2} g(\alpha', Q) \sin(\alpha') d\alpha' \right\} d\beta'}, \quad (10a)$$

$$g(\alpha, Q) := \exp \left[ - \frac{(\alpha - Q)^2}{2\varpi^2} \right]. \quad (10b)$$

## 4 Principle of Virtual Powers and Field Equations

In the model developed by Olsson and Klarbring [53] for the reorientation of fibres in arteries, the law governing the time-dependent alignment of the fibres was deduced from the Principle of Virtual Powers and the Principle of Maximum Dissipation. The model was based on the theories developed by DiCarlo and Quiligotti [14] for tissue growth, Cermelli et al. [8] for rate-independent plasticity, and Gurtin [33] for a generalisation of the Allen-Cahn and Cahn-Hilliard models. Although these theories were conceived for quite different modelling purposes, they have common features and —to the best of our understanding— their most relevant aspects are the treatment of kinematics and the concept of force (a linear, continuous, real-valued functional defined on the set of test velocities, cf. DiCarlo and Quiligotti [14]). In summary, a body undergoing both changes of shape and transformations of internal structure necessitates two types of independent kinematic descriptors: the first type is given by the velocity  $\mathbf{v}$  (or  $\mathbf{u}$ ); the second type comprehends the descriptors associated with the body structural changes. In the problem analysed by Olsson and Klarbring [53], the kinematic descriptors of the second type were the angular velocities with which the fibres reoriented.

It is important to remark that, in the framework outlined above, the structural descriptors

are not treated as the rates of internal variables. Rather, they are viewed as generalised velocities that, as such, must be power-conjugate to properly defined generalised forces. These forces must, in turn, satisfy balance laws.

In the following, a purely mechanical context is considered and only the structural reorganisation due to the reorientation of fibres is studied. Moreover, the structural change of the composite material under investigation is characterised by a single kinematic descriptor, which is referred to as “remodelling variable”, whereas its power-conjugate forces are said to be “remodelling forces”. These can be both internal and external, and are required to satisfy a balance law. Under suitable hypotheses, the internal forces are determined constitutively, and it is shown that they feature a dissipative contribution that is related to the remodelling variable.

While the methods discussed above supply the bases for our theory, our paper addresses the structural reorganisation of statically oriented composites. To this end, the kinematic descriptor of remodelling chosen in our approach is the generalised velocity  $\Omega := \dot{Q}$ , i.e., the time derivative of the angle  $Q$  that parameterises the PDD (10a), and determines the most probable direction along which the fibres are aligned at a given point  $X \in \mathcal{C}$  and instant of time  $t \in [0, t_f]$ .

Formally, the set of kinematic descriptors of the body under consideration may be defined as

$$\mathcal{G} := \{(\mathbf{u}, \Omega) : \mathcal{C} \times [t_0, t_f] \rightarrow T\mathcal{E} \times \mathbb{R} \mid \mathbf{u} = \dot{\chi}^a \mathbf{e}_a, \text{ and } \Omega = \dot{Q}\}, \quad (11)$$

where  $\{\mathbf{e}_a\}_{a=1}^3$  is a vector basis in  $T\mathcal{E}$ . Here,  $\Omega$  is assumed to belong to  $L^2(\mathcal{C}, \mathbb{R})$ , i.e., the Lebesgue space of real-valued, square-integrable functions over  $\mathcal{C}$ , whereas  $\mathbf{u}$  is an element of the Sobolev space  $(H^1(\mathcal{C}))^3 := \{\mathbf{w} \in (L^2(\mathcal{C}, T\mathcal{E}))^3 \mid \text{Grad} \mathbf{w} \in (L^2(\mathcal{C}, T\mathcal{E}))^{3,3}\}$ , i.e., the set of all vector fields  $\mathbf{w}$ , defined in  $\mathcal{C}$  and valued in  $T\mathcal{E}$ , that are square-integrable over  $\mathcal{C}$  and whose first derivatives in the sense of distribution are square-integrable over  $\mathcal{C}$  too [57].

The set of generalised virtual (test) velocities is the collection of all admissible realisations

$$\tilde{\mathcal{G}} := \{(\tilde{\mathbf{u}}, \tilde{\Omega}) : \mathcal{C} \times [t_0, t_f] \rightarrow T\mathcal{E} \times \mathbb{R} \mid \tilde{\mathbf{u}}|_{\partial\mathcal{C}_D} = \mathbf{0}\}, \quad (12)$$

where  $\tilde{\mathbf{u}}|_{\partial\mathcal{C}_D}$  is the restriction of  $\tilde{\mathbf{u}}$  to the Dirichlet boundary of  $\mathcal{C}$  (i.e., the portion of the boundary

where position boundary conditions are imposed). The test velocity  $\tilde{\mathbf{u}}$  is an element of the space  $(H_0^1(\mathcal{C}))^3 = \{\tilde{\mathbf{w}} \in (H^1(\mathcal{C}))^3 \mid \tilde{\mathbf{w}}|_{\partial\mathcal{C}_D} = \mathbf{0}\}$ .

The virtual power done by external forces is defined by the linear functional  $\mathcal{P}_e : \tilde{\mathcal{G}} \rightarrow \mathbb{R}$ ,

$$\mathcal{P}_e(\tilde{\mathbf{u}}, \tilde{\Omega}) := \underbrace{\int_{\mathcal{C}} \mathbf{b} \cdot \tilde{\mathbf{u}} + \int_{\partial\mathcal{C}_N} \mathbf{f} \cdot \tilde{\mathbf{u}}}_{\text{Standard terms}} + \underbrace{\int_{\mathcal{C}} Z_e \tilde{\Omega}}_{\text{Remodelling}}. \quad (13)$$

In (13),  $\mathbf{b}$  groups together all body forces per unit volume of the reference configuration (i.e., inertia and long-range interactions),  $\mathbf{f}$  denotes contact forces measured per unit area of the Neumann-boundary  $\partial\mathcal{C}_N$ , i.e., the portion of the boundary where traction boundary conditions are imposed), and  $Z_e$  comprehends all remodelling forces due to interactions of the body with its environment. In some biomechanical applications of tissue remodelling, forces of this kind are identified with the target values of the internal forces that drive the structural reorganisation of the considered tissues. In some cases, the introduction of these target forces facilitates the determination of the stationary states of the studied remodelling processes. More details about this issue and its connection with our work shall be outlined in section 5.

The virtual power done by the internal forces is defined by the linear functional  $\mathcal{P}_i : \tilde{\mathcal{G}} \rightarrow \mathbb{R}$ ,

$$\mathcal{P}_i(\tilde{\mathbf{u}}, \tilde{\Omega}) := \underbrace{\int_{\mathcal{C}} \text{tr}[\mathbf{P}(\mathbf{g} \text{Grad} \tilde{\mathbf{u}})^T]}_{\text{Standard term}} + \underbrace{\int_{\mathcal{C}} Z_i \tilde{\Omega}}_{\text{Remodelling}}. \quad (14)$$

In (14),  $\mathbf{P}$  is the first Piola-Kirchhoff stress tensor, and  $Z_i$  is the internal remodelling force. The physical meaning and the functional form of  $Z_i$  are discussed in section 5. The assumption of incompressibility, as stated in (7), implies that  $\mathbf{P}$  takes the form

$$\mathbf{P} = \mathbf{P}_v + \mathbf{P}_d = -Jp\mathbf{g}^{-1}\mathbf{F}^{-T} + \mathbf{P}_d, \quad (15)$$

where  $\mathbf{P}_v = -Jp\mathbf{g}^{-1}\mathbf{F}^{-T}$  and  $\mathbf{P}_d$  are, respectively, the volumetric and distortional parts of  $\mathbf{P}$ , and the hydrostatic pressure  $p$  is the Lagrange multiplier associated with (7). Furthermore, the space  $\tilde{\mathcal{P}} \subset L^2(\mathcal{C}, \mathbb{R})$  of virtual pressures  $\tilde{p}$  is introduced, and the constrained virtual power  $\mathcal{P}_c : \tilde{\mathcal{P}} \rightarrow \mathbb{R}$  is

276 defined as

$$\mathcal{P}_c(\tilde{p}) := - \int_{\mathcal{C}} \text{tr}[J\tilde{p}(\text{Grad}\mathbf{u})\mathbf{F}^{-1}]. \quad (16)$$

277 The Principle of Virtual Powers can be expressed by means of the condition [36]

$$\mathcal{P}_e(\tilde{\mathbf{u}}, \tilde{\Omega}) = \mathcal{P}_i(\tilde{\mathbf{u}}, \tilde{\Omega}) + \mathcal{P}_c(\tilde{p}). \quad (17)$$

278 By substituting (13)–(16) into (17), using the relation  $\text{tr}[\mathbf{P}(\mathbf{g}\text{Grad}\tilde{\mathbf{u}})^T] = \text{Div}(\mathbf{P}^T.\tilde{\mathbf{u}}) - \text{Div}(\mathbf{P}).\tilde{\mathbf{u}}$ ,  
 279 applying Gauss' Theorem, and invoking a well-established localisation argument, one obtains

$$\text{Div}(\mathbf{P}) + \mathbf{b} = \mathbf{0}, \quad \text{in } \mathcal{C}, \quad (18a)$$

$$\mathbf{P}.\mathbf{N} = \mathbf{f}, \quad \text{on } \partial\mathcal{C}_N, \quad (18b)$$

$$\text{tr}[J(\text{Grad}\mathbf{u})\mathbf{F}^{-1}] = 0, \quad \text{in } \mathcal{C}, \quad (18c)$$

$$Z_i = Z_e, \quad \text{in } \mathcal{C}. \quad (18d)$$

280 The equations to be solved are (18a), (18c), and (18d). These constitute a set of five independent  
 281 equations. The functional form of the forces  $\mathbf{b}$ ,  $\mathbf{f}$  and  $Z_e$  is assumed to be given from the outset,  
 282 while  $\mathbf{P}_d$  and  $Z_i$  should be specified constitutively. By doing so, one obtains a closed mathematical  
 283 problem consisting of a system of five equations in the five unknowns  $\{\chi^a\}_{a=1}^3$ ,  $p$ , and  $Q$ .

## 284 5 Dissipation and constitutive theory

285 Let  $\mathcal{M} \subset \mathcal{C}$  be a fixed part of  $\mathcal{C}$ . The dissipation associated with  $\mathcal{M}$  is defined by

$$\int_{\mathcal{M}} D = - \overline{\int_{\mathcal{M}} \dot{\Psi}} + \mathcal{P}_n(\mathcal{M}) \geq 0, \quad (19)$$

where  $D$  and  $\Psi$  are, respectively, the dissipation density and stored energy function measured per unit volume of the reference configuration, and  $\mathcal{P}_n(\mathcal{M})$  is referred to as net power, i.e.,

$$\begin{aligned}\mathcal{P}_n(\mathcal{M}) &:= \int_{\partial\mathcal{M}} (\mathbf{P} \cdot \mathbf{N}) \cdot \mathbf{u} + \int_{\mathcal{M}} \mathbf{b} \cdot \mathbf{u} + \int_{\mathcal{M}} Z_e \Omega \\ &= \int_{\mathcal{M}} \text{tr}[\mathbf{P}(\mathbf{g} \text{Grad} \mathbf{u})^T] + \int_{\mathcal{M}} Z_i \Omega.\end{aligned}\tag{20}$$

Since  $\mathcal{M}$  is fixed, it holds true that  $\overline{\dot{\int_{\mathcal{M}} \Psi}} = \int_{\mathcal{M}} \dot{\Psi}$ . Moreover, by using the chain of identities  $\text{tr}[\mathbf{P}(\mathbf{g} \text{Grad} \mathbf{u})^T] = \text{tr}[\mathbf{P}_d(\mathbf{g} \text{Grad} \mathbf{u})^T] = \frac{1}{2} \text{tr}[\mathbf{S}_d \dot{\mathbf{C}}]$ , and localising the result, one obtains

$$D = -\dot{\Psi} + \frac{1}{2} \mathbf{S}_d : \dot{\mathbf{C}} + Z_i \Omega \geq 0.\tag{21}$$

The triples  $(\mathbf{C}, Q, \Omega) \in (T^*\mathcal{C} \otimes T^*\mathcal{C})_S \times \mathbb{R} \times \mathbb{R}$  are the independent constitutive variables of our theory. The angle  $Q$  describes the changes of the most probable direction of local fibres alignment, whereas the velocity  $\Omega$  captures the dissipative aspects of this process.

Constitutive functions must comply with the following requirements: (i) objectivity, (ii) locality, and (iii) criterion of maximum dissipation. Moreover, they are supplied in the form

$$\Psi = \hat{\Psi}(\Phi_f, \mathbf{C}, Q),\tag{22a}$$

$$\mathbf{S}_d = \hat{\mathbf{S}}_d(\Phi_f, \mathbf{C}, Q),\tag{22b}$$

$$Z_i = \hat{Z}_i(\Phi_f, \mathbf{C}, Q, \Omega),\tag{22c}$$

In general, (22c) holds true for all  $\Omega \neq 0$ . It should be remarked that, although the axiomatic theory of constitutive laws prescribes that all dependent constitutive functionals depend on the same list of arguments, the elimination of  $\Omega$  from the list of arguments of  $\hat{\Psi}$  and  $\hat{\mathbf{S}}_d$  does not affect the results determined below.

To be more specific,  $\hat{\Psi}$  and  $\hat{\mathbf{S}}_d$  are required to be continuous with respect to the whole list of their arguments, and  $\hat{\Psi}$  is assumed to be smooth in  $\Phi_f$ ,  $\mathbf{C}$ , and  $Q$ . Moreover,  $\hat{Z}_i$  is prescribed to be bounded and continuous when  $\Omega \neq 0$ , but it is allowed to be constitutively indeterminate when

302  $\Omega$  vanishes.

303 By setting  $\Omega \neq 0$ , and inserting (22) into (21), the dissipation inequality is rewritten as

$$D = \frac{1}{2} \left[ \hat{\mathbf{S}}_d - 2 \frac{\partial \hat{\Psi}}{\partial \mathbf{C}} \right] : \dot{\mathbf{C}} + \left[ \dot{Z}_i - \frac{\partial \hat{\Psi}}{\partial Q} \right] \Omega \geq 0. \quad (23)$$

304 Following the prescription  $\hat{\Psi}(\Phi_f, \mathbf{C}, Q) = \hat{W}(\Phi_f, \mathbf{\Upsilon}(\mathbf{C}), Q)$ , with  $\mathbf{\Upsilon}(\mathbf{C}) = \overline{\mathbf{C}}$  [6], the distortional  
 305 part of the second Piola-Kirchhoff stress tensor is defined constitutively by

$$\mathbf{S}_d = \hat{\mathbf{S}}_d(\Phi_f, \mathbf{C}, Q) = [\det(\mathbf{C})]^{-1/3} \mathbb{M}(\mathbf{C}) : \left( 2 \frac{\partial \hat{W}}{\partial \overline{\mathbf{C}}}(\Phi_f, \overline{\mathbf{C}}, Q) \right). \quad (24)$$

306 To obtain the expression of the total second Piola-Kirchhoff stress tensor, the volumetric part  
 307  $\mathbf{S}_v = -Jp\mathbf{B}$  must be added to  $\mathbf{S}_d$ . Since  $J$  is equal to unity, it follows that  $\mathbf{B} = \overline{\mathbf{B}}$ , and  $\mathbf{S}$  becomes

$$\mathbf{S} = \mathbf{S}_v + \mathbf{S}_d = -p\overline{\mathbf{B}} + \mathbb{M}(\overline{\mathbf{C}}) : \left( 2 \frac{\partial \hat{W}}{\partial \overline{\mathbf{C}}}(\Phi_f, \overline{\mathbf{C}}, Q) \right). \quad (25)$$

308 By introducing the dissipative remodelling force

$$Y := Z_i - \frac{\partial \hat{W}}{\partial Q}, \quad (26)$$

309 the dissipation inequality (23) reduces to  $D = Y\Omega \geq 0$ , whenever  $\Omega \neq 0$ . Since dissipation has  
 310 to vanish when  $\Omega$  is null, but the force  $Y$  might be constitutively indeterminate in this case, one  
 311 arrives at

$$D = Y\Omega = \begin{cases} \hat{Y}(\Phi_f, \overline{\mathbf{C}}, Q, \Omega) \Omega \geq 0, & \text{if } \Omega \neq 0, \\ 0, & \text{if } \Omega = 0. \end{cases} \quad (27)$$

312 The scope of the study of the residual dissipation inequality is to individuate a constitutive law  
 313  $Y = \hat{Y}(\Phi_f, \overline{\mathbf{C}}, Q, \Omega)$  that is in harmony with the criterion of maximum dissipation. When this law  
 314 can be found, the force balance (18d) yields

$$\hat{Y}(\Phi_f, \overline{\mathbf{C}}, Q, \Omega) = Z_e - \frac{\partial \hat{W}}{\partial Q}(\Phi_f, \overline{\mathbf{C}}, Q). \quad (28)$$



315 Since the functional forms of  $\hat{Y}$  and  $\hat{W}$  are provided constitutively and the interaction  $Z_e$  is known  
 316 from the outset, the parameter  $Q$  can be determined by solving (28). Once the variables  $Q$  and  $\Omega$   
 317 are known, the remodelling force  $Z_i$  can be expressed by means of (26).

318 As remarked by Cermelli et al. [8], when  $Z_e$  is zero or negligibly small, the force balance (18d)  
 319 implies that the internal force  $Z_i$  is zero too, which, in turn, implies that  $\hat{Y}$  is given by

$$\hat{Y}(\Phi_f, \bar{\mathbf{C}}, Q, \Omega) = -\frac{\partial \hat{W}}{\partial Q}(\Phi_f, \bar{\mathbf{C}}, Q). \quad (29)$$

## 320 5.1 Elastic strain energy function and stress

321 The fibre-reinforced composite material under investigation is assumed to be hyperelastic. Follow-  
 322 ing Federico and Grillo [21], the elastic strain energy density of the material is constructed by  
 323 superposing the elastic contribution of the matrix to that of the fibres, i.e.,

$$\hat{W}(\Phi_f, \bar{\mathbf{C}}, Q) = (1 - \Phi_f)\hat{W}_m(\bar{\mathbf{C}}) + \Phi_f\hat{W}_f(\bar{\mathbf{C}}, Q), \quad (30)$$

324 where  $\hat{W}_m$  and  $\hat{W}_f$  denote the stored energy functions of the matrix and fibres, respectively. The  
 325 combination (30) is based on the assumption that the matrix consists of an isotropic material  
 326 whose mechanical behaviour does not depend on  $Q$ . Due to incompressibility, the stored energy  
 327 function defined in (30) is taken to be independent of the volumetric part of deformation in order  
 328 to ensure that the volumetric part of stress remains constitutively indeterminate [61]. Moreover,  
 329 the dependence of  $\hat{W}$  on  $\Phi_f$  and  $Q$  accounts for the micro-structural contribution of the composite  
 330 to the overall energy.

331 The energy  $\hat{W}_f$  is written as the sum of an isotropic and an anisotropic contribution, i.e.,

$$\hat{W}_f(\bar{\mathbf{C}}, Q) = \hat{W}_{fi}(\bar{\mathbf{C}}) + \hat{W}_{fa}(\bar{\mathbf{C}}, Q). \quad (31)$$

332 The energy  $\hat{W}_{fa}$  represents the sum of all contributions given by the fibres to the elastic energy of  
 333 the composite. Since the fibres are assumed to be oriented statistically, as described by the PDD

334  $\wp$ ,  $\hat{W}_{fa}$  can be defined as follows

$$\hat{W}_{fa}(\bar{\mathbf{C}}, Q) = \int_{\mathbb{H}^2} \wp(\mathbf{M}, Q) \hat{w}_{fa}(\bar{\mathbf{C}}, \mathbf{A}(\mathbf{M})) dS, \quad (32)$$

335 where  $\mathbf{A}(\mathbf{M}) := \mathbf{M} \otimes \mathbf{M}$  is the structure tensor attached at  $X$ , and  $\hat{w}_{fa}$  is the stored energy  
336 function contributed by those fibres that are aligned along  $\mathbf{M}$ .

337 If the fibres are regarded to be active only when they are stretched,  $\hat{w}_{fa}$  can be written as

$$\hat{w}_{fa}(\bar{\mathbf{C}}, \mathbf{A}(\mathbf{M})) = \mathcal{H}(I_4(\bar{\mathbf{C}}, \mathbf{A}(\mathbf{M})) - 1) \hat{w}_{fb}(\bar{\mathbf{C}}, \mathbf{A}(\mathbf{M})), \quad (33)$$

338 where  $\hat{w}_{fb}$  is the “actual” contribution to the elastic energy of the fibres aligned along  $\mathbf{M}$ , the  
339 invariant  $I_4(\bar{\mathbf{C}}, \mathbf{A}(\mathbf{M}))$  is given by  $I_4(\bar{\mathbf{C}}, \mathbf{A}(\mathbf{M})) = \text{tr}(\bar{\mathbf{C}}\mathbf{A}(\mathbf{M}))$ , and  $\mathcal{H}(\cdot)$  is the Heaviside distri-  
340 bution (it returns one when its argument is strictly positive, and zero otherwise). In this paper,  
341  $\hat{W}_m$ ,  $\hat{W}_{fi}$  and  $\hat{w}_{fb}$  are defined by the expressions

$$\hat{W}_m(\bar{\mathbf{C}}) = \frac{1}{2} c_m [I_1(\bar{\mathbf{C}}) - 3], \quad (34a)$$

$$\hat{W}_{fi}(\bar{\mathbf{C}}) = \frac{1}{2} c_{fi} [I_1(\bar{\mathbf{C}}) - 3], \quad (34b)$$

$$\hat{w}_{fb}(\bar{\mathbf{C}}, \mathbf{A}(\mathbf{M})) = \frac{1}{4} c_{fb} [I_4(\bar{\mathbf{C}}, \mathbf{A}(\mathbf{M})) - 1]^2, \quad (34c)$$

342 where  $c_m$ ,  $c_{fi}$ , and  $c_{fb}$  are material constants, and  $I_1(\bar{\mathbf{C}}) = \text{tr}(\mathbf{G}^{-1}\bar{\mathbf{C}})$ . Thus, the differentiation of  
343  $\hat{W}$  with respect to  $\mathbf{C}$  yields the distortional part of the second Piola-Kirchhoff stress tensor, i.e.,

$$\begin{aligned} \mathbf{S}_d &= c(\Phi_f) [\mathbf{G}^{-1} - \frac{1}{3} I_1(\bar{\mathbf{C}}) \bar{\mathbf{C}}^{-1}] \\ &+ \int_{\mathbb{H}_0^2(\bar{\mathbf{C}})} \wp(\mathbf{M}, Q) \zeta(\Phi_f, \bar{\mathbf{C}}, \mathbf{A}(\mathbf{M})) \hat{\mathbf{A}}_d(\mathbf{M}, \bar{\mathbf{C}}) dS, \end{aligned} \quad (35)$$

344 where the following notation has been introduced:

$$c(\Phi_f) := (1 - \Phi_f)c_m + \Phi_f c_{fi}, \quad (36a)$$

$$\zeta(\Phi_f, \overline{\mathbf{C}}, \mathbf{A}(\mathbf{M})) := \Phi_f c_{fb} [I_4(\overline{\mathbf{C}}, \mathbf{A}(\mathbf{M})) - 1], \quad (36b)$$

$$\hat{\mathbf{A}}_d(\mathbf{M}, \overline{\mathbf{C}}) := \mathbf{A}(\mathbf{M}) - \frac{1}{3} I_4(\overline{\mathbf{C}}, \mathbf{A}(\mathbf{M})) \overline{\mathbf{B}}, \quad (36c)$$

$$\mathbb{H}^2 \supset \mathbb{H}_0^2(\overline{\mathbf{C}}) := \{\mathbf{M} \in \mathbb{H}^2 \mid I_4(\overline{\mathbf{C}}, \mathbf{A}(\mathbf{M})) > 1\}. \quad (36d)$$

## 345 5.2 Principle of Maximum Dissipation

346 The results reported in this section follow closely the theory developed by Hackl and Fischer[34].

347 In the residual dissipation inequality (27),  $D$  is assumed to admit the constitutive form

$$D = \hat{D}(\Lambda, \Omega) \geq 0, \quad (37)$$

348 where  $\Lambda := (\Phi_f, \overline{\mathbf{C}}, Q)$  collects all variables other than  $\Omega$ . Our hypotheses are that  $\hat{D}(\Lambda, \Omega)$  is zero  
 349 at  $\Omega = 0$ , that  $\hat{D}$  is continuous for all  $\Lambda$  and for all real values of  $\Omega$ , but differentiable only for  
 350  $\Omega \neq 0$ , and that  $\hat{D}$  can be expressed as a homogeneous function of degree  $n \in \mathbb{N}$  with respect to  
 351  $\Omega$ , i.e.,  $\hat{D}(\Lambda, \alpha\Omega) = \alpha^n \hat{D}(\Lambda, \Omega)$  for all values of  $\Omega$ , and for all  $\alpha > 0$ .

352 If the requisite  $\Omega \neq 0$  is fulfilled, an expression defining  $Y$  constitutively, i.e.,  $Y = \hat{Y}(\Lambda, \Omega)$ , is  
 353 sought for. This expression maximises the dissipation over the space of all admissible velocities  $\Omega$ .  
 354 To achieve this result under the condition that  $\hat{D}$  maintains the structure  $\hat{D}(\Lambda, \Omega) = Y\Omega$  (cf. (27)  
 355 and Hackl and Fisher [34] for explanations about this issue), a constrained optimisation problem  
 356 has to be solved. This is done by setting equal to zero the partial derivatives of

$$\hat{L}(\Lambda, \Omega, \gamma) := \hat{D}(\Lambda, \Omega) + \gamma[\hat{D}(\Lambda, \Omega) - Y\Omega], \quad (38)$$

357 where  $\hat{L}$  is the Lagrangian function of the constrained optimisation problem, and  $\gamma$  is an unknown

358 Lagrangian multiplier. This procedure leads to:

$$\frac{\partial \hat{L}}{\partial \Omega}(\Lambda, \Omega, \gamma) = (1 + \gamma) \frac{\partial \hat{D}}{\partial \Omega}(\Lambda, \Omega) - \gamma Y = 0, \quad (39a)$$

$$\frac{\partial \hat{L}}{\partial \gamma}(\Lambda, \Omega, \gamma) = \hat{D}(\Lambda, \Omega) - Y\Omega = 0. \quad (39b)$$

359 Solving the set (39) for  $\gamma$  and  $Y$  yields

$$\gamma = \gamma_n = \frac{n}{1 - n}, \quad n \neq 1, \quad (40a)$$

$$Y = \hat{Y}_n(\Lambda, \Omega) = \frac{1}{n} \frac{\partial \hat{D}}{\partial \Omega}(\Lambda, \Omega). \quad (40b)$$

360 When the degree of homogeneity of the dissipation function is unitary (e.g., for rate-independent  
361 materials), the multiplier  $\gamma_n$  is not defined. In this case, (40b) is valid as long as  $\Omega \neq 0$  holds true,  
362 since  $Y$  is constitutively indeterminate at  $\Omega = 0$ .

### 363 5.3 Rate-dependent remodelling

364 We assume here that the dissipation function (37) admits the form

$$\hat{D}(\Lambda, \Omega) = \hat{Y}(\Lambda, \Omega)\Omega \geq 0, \quad (41)$$

365 where  $\hat{Y}(\Lambda, \Omega)$  is constitutively determinate at  $\Omega = 0$ . Moreover, we require that  $\hat{Y}(\Lambda, \Omega)$  vanishes  
366 for vanishing  $\Omega$ , which implies the even stronger condition  $\hat{Y}(\Lambda, 0) = 0$ , for all  $\Lambda$ . Conditions  
367 of this type can be found in the derivation of Fourier's law of heat conduction, e.g., [17]. These  
368 derivations meet the characterisation of thermodynamic equilibrium of Glansdorff and Prigogine  
369 [30] and Rajagopal and Srinivasa [54], which requires both flux-like variables and affinities to be  
370 zero. In the theory presented in our work, the flux-like variable is the remodelling force  $Y$ , while  
371 the affinity is the velocity  $\Omega$ .

372 In the cases in which a linearisation of the constitutive function  $\hat{Y}(\Lambda, \Omega)$  in a neighbourhood of

373  $\Omega = 0$  is physically acceptable, the force  $Y$  may be assigned through the constitutive expression

$$\hat{Y}(\Lambda, \Omega) = \Gamma(\Lambda)\Omega, \quad (42)$$

374 where  $\Gamma(\Lambda)$  is a positive function of  $\Lambda$ . Substitution of (42) into (41) leads to define the dissipation  
 375 as a positive definite quadratic function of  $\Omega$ , i.e.,  $\hat{D}(\Lambda, \Omega) = \Gamma(\Lambda)\Omega^2$ . Since a function of this type  
 376 is homogeneous of degree two with respect to  $\Omega$ , the formula (40b) yields (42).

377 Substituting (42) into the force balance (28) leads to the evolution equation for  $Q$ , i.e.

$$\Gamma(\Phi_f, \overline{\mathbf{C}}, Q)\Omega = Z_e - \frac{\partial \hat{W}}{\partial Q}(\Phi_f, \overline{\mathbf{C}}, Q). \quad (43)$$

378 Equations (43), (18a) and (18b), equipped with initial conditions, describe the problem of remod-  
 379 elling in a fibre-reinforced material. When  $Z_e$  is identically zero, the condition  $\Omega = 0$ , which implies  
 380 the vanishing of the left-hand side of (43), is attained for those physically meaningful values of  $Q$   
 381 solving the stationary problem

$$-\frac{\partial \hat{W}}{\partial Q}(\Phi_f, \overline{\mathbf{C}}, Q) = 0. \quad (44)$$

382 For given  $\Phi_f$  and  $\overline{\mathbf{C}}$ , the existence of stationary points of  $\hat{W}(\Phi_f, \overline{\mathbf{C}}, \cdot)$  restricts the choice of the  
 383 admissible forms of the strain energy function.

## 384 5.4 Remodelling force

385 In order to evaluate the evolution of the remodelling variable  $Q$  according to (43), we have to  
 386 compute the derivative of the Helmholtz free energy density  $\hat{W}$  with respect to  $Q$ . Looking at the  
 387 definition of  $\wp$  given in (10a) and at the form of  $\hat{W}$  given in (34), we notice that  $\hat{W}$  depends on  $Q$   
 388 through  $\wp$ .

389 By plugging (10b) into (30), we obtain

$$\frac{\partial \hat{W}}{\partial Q}(\Phi_f, \overline{\mathbf{C}}, Q) = \Phi_f \int_{\mathbb{H}_0^2(\overline{\mathbf{C}})} \frac{\partial \wp}{\partial Q}(\mathbf{M}, Q) \hat{w}_{fb}(\overline{\mathbf{C}}, \mathbf{A}(\mathbf{M})) d\mathbf{S}, \quad (45)$$

390 where

$$\frac{\partial \wp}{\partial Q}(\alpha, Q) = \wp(\alpha, Q) \frac{\alpha - \langle \alpha \rangle(Q)}{\varpi^2}, \quad (46)$$

391 and  $\langle \alpha \rangle$  denotes the directional (statistical) average of  $\alpha$ . For any function  $\mathbf{f}$  defined on the unit  
392 hemisphere, the directional average of  $\mathbf{f}$  is defined by:

$$\langle \mathbf{f} \rangle(Q) := \int_{\mathbb{H}^2} \wp(\mathbf{M}, Q) \mathbf{f}(\mathbf{M}) d\mathbf{S}. \quad (47)$$

393 With this notation, the derivative (45) can be written in compact form as

$$\frac{\partial \hat{W}}{\partial Q}(\Phi_f, \overline{\mathbf{C}}, Q) = \Phi_f \frac{\langle \alpha \hat{w}_{fa} \rangle(\overline{\mathbf{C}}, Q) - \langle \alpha \rangle(Q) \langle \hat{w}_{fa} \rangle(\overline{\mathbf{C}}, Q)}{\varpi^2}. \quad (48)$$

## 394 6 Study of a benchmark problem

395 In order to test the approach proposed above, we propose a modified version of the benchmark  
396 problem solved by Olsson and Klarbring [53]. The problem, originally conceived for studying re-  
397 modelling in arteries, considered a fibre-reinforced, thick-walled, growing cylindrical body made of  
398 hyperelastic material and subjected to pure inflation. The problem was axial symmetric and was  
399 solved under the constraint of isochoric elastic deformations.

400 We made four main modifications to the original problem. The first one deals with the general  
401 approach to remodelling, since our composite material is reinforced by statistically oriented fibres,  
402 whereas the composite material studied by Olsson and Klarbring [53] features a given pattern  
403 of fibre orientation. Secondly, we do not consider growth here. Thirdly, we do not specifically  
404 study remodelling in blood vessels (we recall that the PDD defined in (10), on which the following  
405 calculations are based, was introduced for studying articular cartilage [22, 23]). Finally, we set the  
406 external remodelling force equal to zero (this choice and its consequences are discussed below).

407 In the present framework, the body forces  $\mathbf{b}$  are disregarded, and the equation that governs  
408 remodelling is given by (43), with  $\Gamma$  being a known, strictly positive constant. An essential differ-  
409 ence with respect to the paper by Olsson and Klarbring [53] is that, in our approach, the external

remodelling force  $Z_e$  is switched off from the outset (i.e.,  $Z_e = 0$ ). Because of the balance of remodelling forces (18d), this amounts to say that the internal remodelling force  $Z_i$  vanishes identically too and, consequently, the dissipative force, which is constitutively determined by (42), is compensated by the derivative of the stored energy function with respect to  $Q$  (cf. (29)). In this case, the balance laws (18a)–(18d), augmented with an initial condition for  $Q$ , become

$$\text{Div}(\mathbf{P}) = \mathbf{0}, \quad \text{in } \mathcal{C}, \quad (49a)$$

$$\mathbf{P} \cdot \mathbf{N} = \mathbf{f}, \quad \text{on } \partial\mathcal{C}_N, \quad (49b)$$

$$J = 1, \quad \text{in } \mathcal{C}, \quad (49c)$$

$$\Gamma \dot{Q} = -\frac{\partial \hat{W}}{\partial Q}, \quad \text{in } \mathcal{C}, \quad (49d)$$

$$Q(X, 0) = Q_0(X), \quad \text{in } \mathcal{C}. \quad (49e)$$

## 6.1 Deformation under the incompressibility constraint

The coordinates parameterising the reference configuration,  $\mathcal{C}$ , are denoted by  $(R, \Theta, Z)$ , with  $R \in [R_i, R_o]$ ,  $\Theta \in [0, 2\pi]$  and  $Z \in [0, L]$ . Here,  $R_i$  and  $R_o$  are the values of the inner and outer radius of the cross-section of the body, and  $L$  is the axial length of the cylinder. The coordinates associated with the current configuration are indicated by  $(r, \vartheta, z)$ . Since the deformation is assumed to be a pure inflation, we obtain

$$(R, \Theta, Z) \mapsto (r, \vartheta, z) = (\chi^r(R, t), \Theta, Z). \quad (50)$$

For notational convenience, it is set  $\chi^r \equiv \xi$  from here on, and  $\xi'$  denotes the derivative  $\partial\chi^r/\partial R$ .

With respect to the orthonormal bases  $\{\mathbf{E}_R, \mathbf{E}_\Theta, \mathbf{E}_Z\}$  and  $\{\mathbf{e}_r, \mathbf{e}_\vartheta, \mathbf{e}_z\}$ , which are associated with the reference and current configuration, respectively, the deformation gradient is expressed by

$$\mathbf{F} = \xi' \mathbf{e}_r \otimes \mathbf{E}^R + \frac{\xi}{R} \mathbf{e}_\vartheta \otimes \mathbf{E}^\Theta + \mathbf{e}_z \otimes \mathbf{E}^Z. \quad (51)$$

Because of incompressibility, the radial deformation  $\xi$  has to comply with the constraint  $\det(\mathbf{F}) = 1$ ,

426 which results into the differential equation with separable variables

$$\xi'(R, t)\xi(R, t) = R. \quad (52)$$

427 This condition determines  $\xi$  up to an unknown function of time  $K$ , i.e.,

$$\xi(R, t) = \sqrt{R^2 + K(t)}. \quad (53)$$

## 428 6.2 Boundary conditions

429 The boundary of the current configuration is given by  $\partial\mathcal{C}_t = \partial\mathcal{C}_{to} \cup \partial\mathcal{C}_{ti}$ , where the subscripts “o”  
430 and “i” define the “outer” and “inner” surface of the inflated cylinder, respectively. The boundary  
431 conditions are written as

$$\boldsymbol{\tau}|_o = -\lambda_o \mathbf{n}_o \quad \text{on } \partial\mathcal{C}_{to}, \quad \boldsymbol{\tau}|_i = -\lambda_i \mathbf{n}_i \quad \text{on } \partial\mathcal{C}_{ti}, \quad (54)$$

432 where  $\boldsymbol{\tau}$  denotes the distribution of imposed contact forces,  $\mathbf{n}_o \equiv \mathbf{e}_r(r_o, t)$  and  $\mathbf{n}_i \equiv -\mathbf{e}_r(r_i, t)$   
433 are the unit vectors normal to the outer and inner walls, respectively, and  $\lambda_o$  and  $\lambda_i$  are scalar  
434 constants having the physical dimensions of pressure. With these boundary conditions,  $\partial\mathcal{C}_t$  and  
435  $\partial\mathcal{C}$  are entirely Neumann boundaries.

436 The force  $\mathbf{f}$  featuring in (49b), and defined per unit surface of the reference configuration  
437 of the body, is given by  $\mathbf{f} = \boldsymbol{\tau} J \sqrt{\mathbf{N} \cdot \mathbf{C}^{-1} \cdot \mathbf{N}}$  [6], where the factor  $J \sqrt{\mathbf{N} \cdot \mathbf{C}^{-1} \cdot \mathbf{N}}$  accounts for the  
438 change of area when passing from the boundary of the current configuration to that of the reference  
439 placement, and  $\boldsymbol{\tau}$  is the contact force defined per unit area of  $\partial\mathcal{C}_t$ . Using Nanson’s formula, and  
440 accounting for incompressibility yield

$$\mathbf{P} \cdot \mathbf{N}|_o = -\lambda_o \mathbf{g}^{-1} \mathbf{F}^{-T} \cdot \mathbf{N}, \quad \text{on } \partial\mathcal{C}_o, \quad (55a)$$

$$\mathbf{P} \cdot \mathbf{N}|_i = -\lambda_i \mathbf{g}^{-1} \mathbf{F}^{-T} \cdot \mathbf{N}, \quad \text{on } \partial\mathcal{C}_i. \quad (55b)$$

441 Under the assumption that the components of the stress tensor do not depend on the coordinates



442  $\Theta$  and  $Z$ , the boundary conditions (55a) and (55b) as well as the symmetry requirement of the  
 443 Cauchy stress tensor,  $\mathbf{P}\mathbf{F}^T = \mathbf{F}\mathbf{P}^T$ , are sufficient to ensure that the only nonzero components of  
 444  $\mathbf{P}$  are  $P^{rR}$  and  $P^{\vartheta\Theta}$ . Therefore, conditions (55a) and (55b) can be reformulated as

$$p(R_o, t) = \lambda_o + \frac{R_o^2}{R_o^2 + K(t)} S_d^{RR}(R_o, t), \quad \text{on } \partial\mathcal{C}_o, \quad (56a)$$

$$p(R_i, t) = \lambda_i + \frac{R_i^2}{R_i^2 + K(t)} S_d^{RR}(R_i, t), \quad \text{on } \partial\mathcal{C}_i. \quad (56b)$$

### 445 6.3 Pressure and time-dependent integration constant $K$

446 Pressure can be determined by solving the balance of momentum

$$\frac{\partial P^{rR}}{\partial R} + \frac{P^{rR} - P^{\vartheta\Theta}}{R} = 0 \quad (57)$$

447 together with (56a) and (56b). Indeed, direct integration of (57) leads to

$$p(R, t) = \left[ \frac{R}{\xi(R, t)} \right]^2 S_d^{RR}(R, t) + \lambda_i(t) - \int_{R_i}^R \frac{1}{\xi(A, t)} \eta(A, t) dA, \quad (58)$$

448 where  $\eta$  is the auxiliary function defined by

$$\eta(A, t) := \frac{\xi(A, t)}{A} S_d^{\Theta\Theta}(A, t) - \left[ \frac{A}{\xi(A, t)} \right]^3 S_d^{RR}(A, t). \quad (59)$$

449 Equation (58) defines pressure up to the (still unknown) function of time  $K$ . To determine  $K$ ,  
 450 the pressure is evaluated at  $R = R_o$ , and the boundary condition (56a) is enforced. Under the  
 451 simplifying assumption  $\lambda_o = 0$ , the following consistency condition is arrived at

$$\lambda_i(t) = \int_{R_i}^{R_o} \frac{1}{\xi(R, t)} \eta(R, t) dR. \quad (60)$$

## 6.4 Initial-boundary-value problem and numerical implementation

The benchmark problem investigated in our work considers a thick-walled cylinder reinforced by fibres, and subjected to a uniformly distributed hydrostatic load applied to the inner wall of the cylinder. At each material point  $X$ , identified by the triple  $(R, \Theta, Z)$ , the direction of the most probable fibre orientation is represented by the unit vector  $\mathbf{M}_p := \sin(Q)\mathbf{E}_R + \cos(Q)\mathbf{E}_Z$ , with  $Q$  being the angle that the symmetry axis of the cylinder (parallel to  $\mathbf{E}_Z$ ) forms with  $\mathbf{M}_p$ . In order to preserve the axial symmetry of the problem, the angle  $Q$  is required to be independent of the tangential coordinate. At the same material point, a generic fibre is aligned along the direction specified by the unit vector  $\mathbf{M} = \sin(\alpha)\cos(\beta)\mathbf{E}_R + \sin(\alpha)\sin(\beta)\mathbf{E}_\Theta + \cos(\alpha)\mathbf{E}_Z$ , where  $\alpha$  is the angle that  $\mathbf{M}$  forms with  $\mathbf{E}_Z$ , and  $\beta$  is the angle that the projection of  $\mathbf{M}$  onto the plane  $\mathbf{E}_R$ - $\mathbf{E}_\Theta$  forms with  $\mathbf{E}_R$ . The set of all space directions emanating from  $X$ ,  $\mathbb{H}^2$ , is obtained by varying  $\alpha \in [0, \pi/2]$  and  $\beta \in [0, 2\pi)$ . Furthermore, the directional distribution of the fibres is governed by the PDD defined in (10), with the parameter  $Q$  satisfying the evolution law (49d). In (49e), the initial distribution  $Q_0(X) = \pi/4$ , for all  $X \in \mathcal{C}$ , is used.

We remark that, in order to simulate the pattern of fibre orientation in an artery, Olsson and Klarbring [53] considered, at each material point  $X$ , two unit vectors  $\mathbf{M}_1$  and  $\mathbf{M}_2$  lying on the plane  $\mathbf{E}_\Theta$ - $\mathbf{E}_Z$ . According to the description given above, the directional distribution of the fibres assumed in our work is different from that considered by Olsson and Klarbring [53].

The initial-boundary value problem (IBVP), given by (49a)–(49e), is reformulated and put in terms of the system of equations (53), (58), (60) and (49d), which determine  $\xi$ ,  $p$ ,  $K$ , and  $Q$ . Equations (53) and (58) can be decoupled from (60) and (49d). Thus, the deformed radius  $\xi$  and the remodelling angle  $Q$  can be determined by solving the subsystem resulting from (60) and (49d). Once  $\xi$  and  $Q$  are known,  $K$  is found by inverting (53), and the pressure  $p$  is provided by (58).

Equations (53), (58), (60) and (49d) are solved numerically for a given initial distribution of the remodelling variable  $Q$ . The solution is based on the remodelling equation (49d), with the angle  $Q$  being treated as primary unknown. Thus, stress, energy, and deformed radius are viewed as functions of  $Q$ . The external remodelling force  $Z_e$  was set equal to zero in our calculations. This ensured that there was no external influence on the remodelling of the system, and that remodelling

480 was purely driven by internal forces.

481 From the numerical point of view, a difficulty arises because the right-hand-side of (49d) ne-  
 482 cessitates, at each time step, the evaluation of the integral given in (45), which, in turn, requires  
 483 the knowledge of the integration set  $\mathbb{H}_0^2(\overline{\mathbf{C}})$ . To specify  $\mathbb{H}_0^2(\overline{\mathbf{C}})$ , we have to detect the subset of the  
 484 unit hemisphere in which the argument of the Heaviside distribution is strictly positive, i.e., we  
 485 have to look for the directions and deformations that satisfy the condition

$$f(\overline{\mathbf{C}}, \mathbf{M}) := I_4(\overline{\mathbf{C}}, \mathbf{A}(\mathbf{M})) - 1 > 0. \quad (61)$$

486 By accounting for (53), and noting that the unit vector  $\mathbf{M}$  depends on the angles  $\alpha$  and  $\beta$ , we can  
 487 rephrase (61) as

$$f(K(t), R, \alpha, \beta) = K \frac{[\sin(\alpha)]^2 [\cos(\beta)]^2}{R^2} \left\{ [\tan(\beta)]^2 - \frac{R^2}{R^2 + K(t)} \right\} > 0. \quad (62)$$

488 If  $K$  is strictly positive (which is consistent with the assumption that the cylinder is being inflated),  
 489 and  $\alpha$  is different from zero, the condition (62) is respected when

$$\beta \in (\beta_0, \pi/2) \cup (\pi/2, \pi - \beta_0) \cup (\pi + \beta_0, 3\pi/2) \cup (3\pi/2, 2\pi - \beta_0), \quad (63)$$

490 with  $\beta_0(R, t) = \arctan[R/\xi(R, t)]$ . Furthermore, we introduce the auxiliary quantity

$$\mathfrak{I}(R, t) := \int_{R_i}^R \frac{1}{\xi(A, t)} \eta(A, t) dA. \quad (64)$$

491 Since  $\xi$  depends on time through  $K$ , while the stresses  $S_d^{RR}$  and  $S_d^{\Theta\Theta}$  depend on time through both  
 492  $K$  and  $Q$ , we may write

$$\mathfrak{I}(R, t) = \hat{\mathfrak{I}}_{A=R_i}^R(K(t), Q(A, t), R), \quad (65)$$

493 where  $\hat{\mathfrak{I}}_{A=R_i}^R$  is a functional of  $Q$ .

494 The material parameters used in our simulations are listed in Table 1. The implementation of

the mathematical problem was performed in MATLAB<sup>®</sup>. The algorithm is presented in Table 2, and amounts to apply the explicit Euler method to the system of equations (53), (58), (60) and (49d). To proceed, we denote by  $t_f$  the final time of observation of the system, and discretize the interval  $[0, t_f]$ , with  $t_f < +\infty$ , by selecting  $(N + 1)$  time instants  $\{t_0, t_1, \dots, t_N\}$ , such that  $t_0 = 0$ ,  $t_N = t_f$  and, for  $n = 0, \dots, (N - 1)$ ,  $t_{n+1} = t_n + \Delta t_n$ , where  $\Delta t_n > 0$  is the length of the subinterval  $\mathcal{I}_{n,n+1} = [t_n, t_{n+1}]$ . In an analogous fashion, the interval  $[R_i, R_o]$  is discretized with a one-dimensional grid of  $(M + 1)$  nodes  $\{R_0, R_1, \dots, R_M\}$ , such that  $R_0 = R_i$ ,  $R_M = R_o$ . The intervals  $\mathcal{J}_{k,k+1} := [R_k, R_{k+1}]$ , with  $k = 0, \dots, (M - 1)$ , are disjoint and cover  $[R_i, R_o]$ . The length of  $\mathcal{J}_{k,k+1}$  is denoted by  $\Delta R_k > 0$ . If  $\psi$  denotes a function that depends on time and radial coordinate, we use the notation  $\psi(R_k, t_n) \equiv \psi_{k,n}$ . We write  $\psi(t_n) \equiv \psi_n$ , when  $\psi$  depends on time only, and  $\psi(R_k) \equiv \psi_k$ , when  $\psi$  depends on the radial coordinate only.

Table 1: Material parameters used in the implementation of the model for the reorientation of fibres in the benchmark problem. The fibres are oriented statistically. To allow for a direct comparison, the parameters were selected to closely approximate the model of Olsson and Klarbring [53]. The parameter  $\Gamma$  was selected equal to unity in order make the evolution speed computable.

Parameter	Value or range	Units
$R_i$	1.0	mm
$R_o$	2.0	mm
$\alpha$	$\in (0, \pi/2)$	rad
$\beta$	$\in (0, 2\pi)$	rad
$\Phi_m$	0.8	—
$\Phi_f$	0.2	—
$c_m$	0.03574	MPa
$c_{fi}$	0.03574	MPa
$c_{fb}$	0.35740	MPa
$\lambda_i$	0.02000	MPa
$\varpi$	0.5	rad
$\Gamma$	1	$\text{N} \cdot \text{m}^{-2} \cdot \text{rad}^{-2} \cdot \text{s}$
$Z_e$	0	$\text{N} \cdot \text{m}^{-2} \cdot \text{rad}^{-1}$
$Q_0$	$\pi/4$	rad

Table 2: The algorithm used for the implementation of the remodelling constitutive model for the remodelling of the fibres in the benchmark problem, with a statistically oriented fibre distribution. The model was implemented in MATLAB<sup>®</sup> due to simplicity of the implementation and the flexibility with array manipulations.

---

<b>GIVEN:</b>		
Discretized radial profile	$R_i \leq R_k \leq R_o, k = 0, \dots, M$	
Inner boundary pressure	$\lambda_i$	
Initial value	$Q_0$	
<b>DO:</b> $n = 1, \dots, N$		
Use the boundary constraint to find	$K(t_n)$	Eq. (60)
Find the deformed radius for all values of	$R$	Eq. (53)
Find the hydrostatic pressure	$p_n$	Eq. (58)
Find the first Piola–Kirchhoff stress	$P_n^{rR}$	
Find the first Piola–Kirchhoff stress	$P_n^{\vartheta\Theta}$	
Find the next time step value of	$Q_{n+1}$	Eq. (69)
<b>END DO</b>		

---

506 In discretized form, the system of equations (60), (53), (58), and (49d) become

$$\lambda_i(t_n) = \hat{\mathcal{J}}_{j=0}^M(K_n, Q_{j,n}, R_o), \quad (66)$$

$$\xi_{k,n} = \sqrt{R_k^2 + K_n}, \quad (67)$$

$$p_{k,n} = \left[ \frac{R_k}{\xi_{k,n}} \right]^2 (S_d^{RR})_{k,n} + \lambda_i(t_n) - \hat{\mathcal{J}}_{j=0}^k(K_n, Q_{j,n}, R_k), \quad (68)$$

$$Q_{k,n+1} = Q_{k,n} + \frac{\Delta t_n}{\Gamma} \left[ (Z_e)_{k,n} - \frac{\partial \hat{W}}{\partial Q}(\Phi_f, \bar{\mathbf{C}}_{k,n}, Q_{k,n}) \right]. \quad (69)$$

507 For a given distribution  $Q_{k,n}$ , the code computes the integration constant  $K_n$ , the deformed radius  
508  $\xi_{k,n}$  and the radial profile of the hydrostatic pressure by solving (66), (67), and (68), respectively.  
509 Determining these quantities allows to calculate the radial profiles of the stresses,  $(S_d^{RR})_{k,n}$  and  
510  $(S_d^{\Theta\Theta})_{k,n}$ . The computed values of  $\xi_{k,n}$  are then substituted into (69) in order to determine  $Q_{k,n+1}$ .  
511 Then, the whole procedure is iterated.

512 All integrals were calculated by using the trapezoidal rule. This could be done because the  
513 integral functions were separable. The deformed radius was calculated by applying a “brute-force”  
514 approach to (66). Even though it would be possible to use the “brute-force” approach for deter-  
515 mining  $K_n$  (rather than  $\xi_{k,n}$ ) from (66), and compute then  $\xi_{k,n}$  analytically from (67), we decided

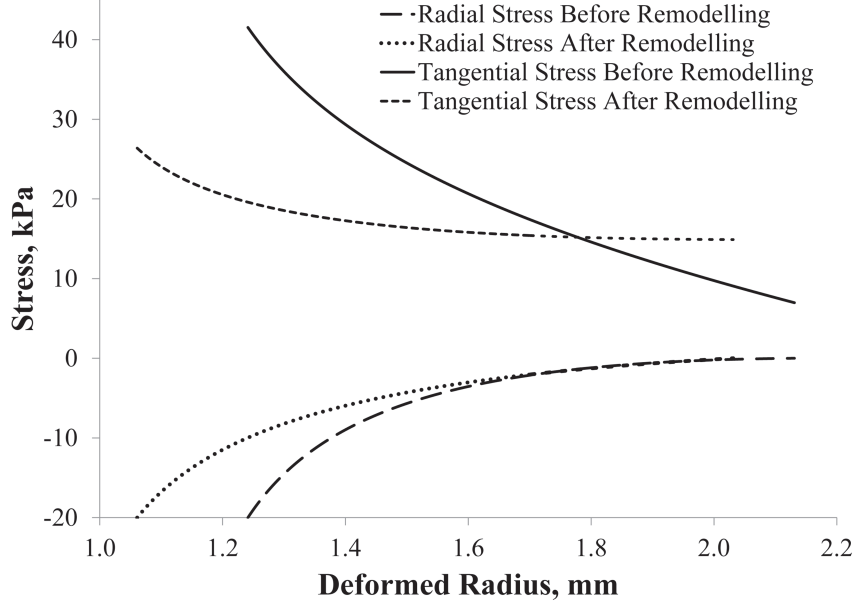


Figure 1: The first Piola–Kirchhoff stress in the radial and tangential directions for the initial loaded configuration and the remodelled configuration.

to implement the inverse path because it is more versatile and easy to extend to more difficult cases without essential modifications to the algorithm.

## 7 Results

The state of stress at each radial point is an important parameter to consider when dealing with remodelling of biological tissues. In the case of the benchmark problem addressed in this paper, the change in both the radial and tangential stresses, before and after remodelling, is plotted versus the deformed radius as depicted in Figure 1. The change in the radial stress is not significant, due to the boundary conditions and the thin profile of the radial geometry. The tangential stress, on the other hand, changes significantly. We observed that, due to the evolution of  $Q$  at different radii, the tangential stress changes non-uniformly with respect to the radius and, in fact, becomes more constant. This is in good agreement with the results of Olsson and Klarbring [53], but

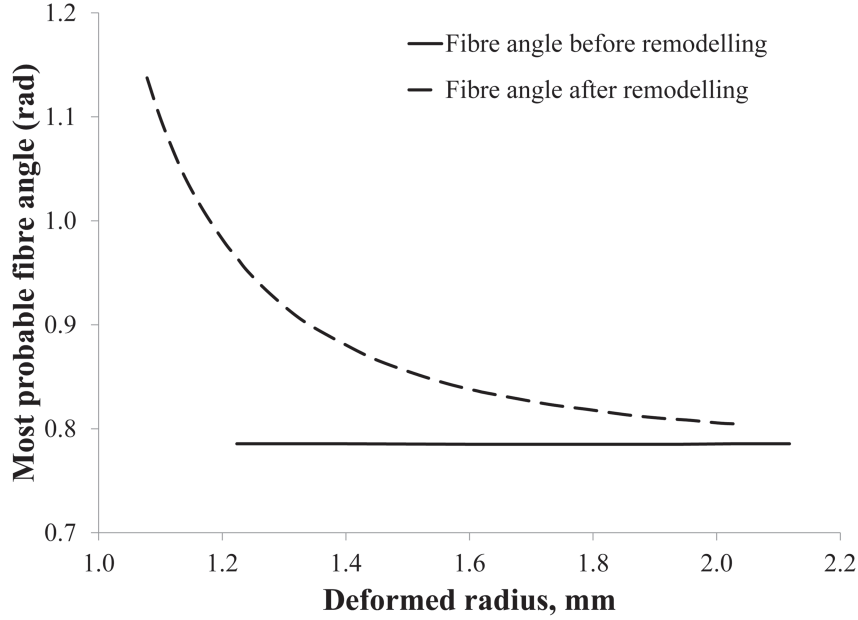


Figure 2: The fibre distribution as a function of the deformed radius, where this angle is formulated as the angle between the fibre direction vector and the axis of symmetry.

there are several differences. Since Olsson and Klarbring [53] modelled growth in addition to fibre remodelling, they observed a slightly different state of tangential stress after remodelling.

Figure 2 depicts  $Q$  as a function of the current radius before and after remodelling. Since the initial value of the most probable angle is constant,  $Q$  is homogeneous before remodelling has occurred. This feature changes when  $Q$  is observed after remodelling, since it becomes quite inhomogeneous. It can be observed that  $Q$  is maximum at the inner surface, and minimum at the outer surface of the hollow cylinder. Since the most probable fibre angle is measured from the symmetry axis, this behaviour might be explained by the fact that, in order to compensate for the higher state of stress at the inner surface, the fibres reorient in a manner that results in higher fibre engagement.

In order to observe the remodelling of the composite material as governed by the remodelling equation, it is important to observe how the most probable fibre angle changes over time. This is shown in Figure 3, which illustrates  $Q$  as a function of time for three different points on the radius:

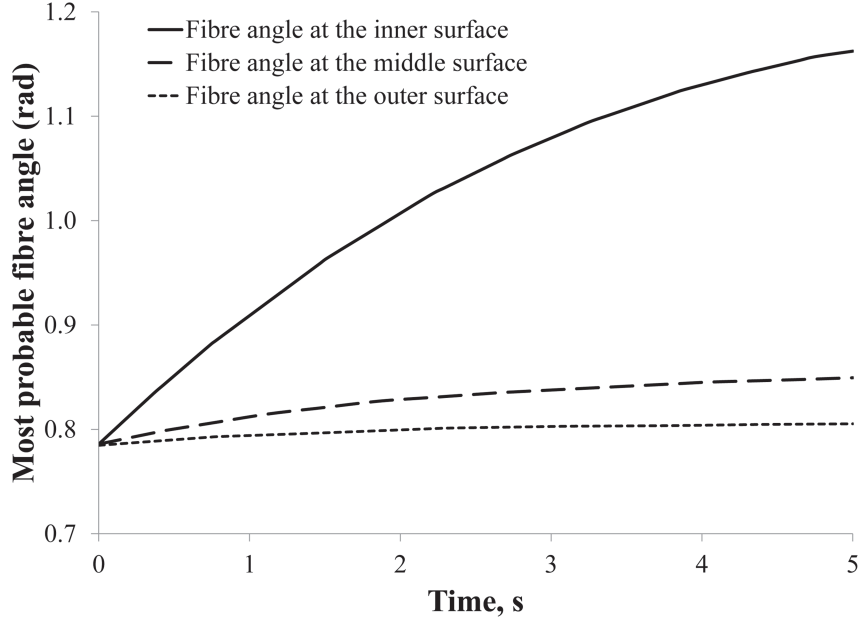


Figure 3: The evolution of the fibre angle over time for three different radii: the inner radius, the outer radius, and the middle radius.

at the inner surface, midway between the inner and the outer surface, and at the outer surface.

The initial value of  $Q$  is the same for all three points on the radius, and that angle was set equal to  $\pi/4$ . As time progresses, the fibre angle evolves differently at each radial point. This can be attributed to the different states of stress at each point, as the stress is one of the driving forces of remodelling. In fact, the tangential stress is highest on the inner surface of the artery studied by Olsson and Klarbring [53], and this is the point at which the mean fibre angle changes the most. Thus, it could be concluded that the fibres attempt to optimise the state of stress through remodelling.

It is also important to note that the mean fibre angle at each radial point is supposed to reach a steady state value, as illustrated in Figure 3. This steady state value represents the optimal fibre orientation. In Figure 3, it can be observed that  $Q$  at the inner surface reaches the steady state the slowest, and this could be attributed to the magnitude of the stress at this material point. In other words, the variation of the most probable fibre angle takes a longer time to reach a steady



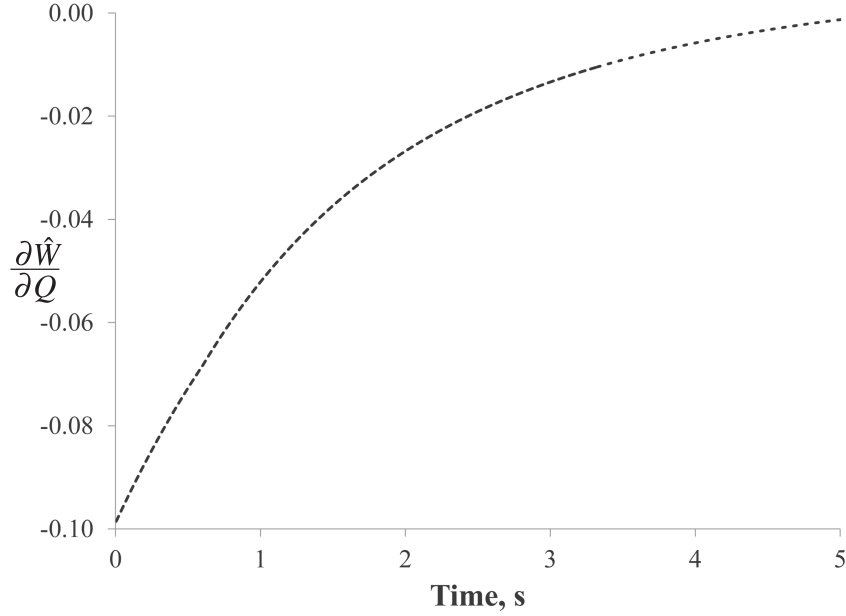


Figure 4: The evolution of the derivative  $\partial \hat{W} / \partial Q$  of the strain energy potential with respect to the remodelling parameter,  $Q$ , over time.

state when there is a large change in the driving force behind remodelling, which is, in this case, stress.

## 8 Discussion and outlook

We studied the structural reorganisation of an incompressible composite material, in which the reinforcing fibres were oriented according to a Gaussian probability distribution. The variance of the Gaussian was given from the outset and assumed to be constant, whereas the angle  $Q$  was taken as the only remodelling variable of the problem. The geometry of the system was taken to be a hollow, thick-walled cylinder.

In addition to the standard balance of momentum, equipped with boundary conditions and the incompressibility constraint, we exploited the Principle of Virtual Powers and the Principle of Maximum Dissipation to determine an admissible constitutive expression for the dissipative force

that drives the reorientation of the fibres. Then, we retrieved the same type of evolution law for the remodelling variable as that found by Olsson and Klarbring [53] and solved numerically the mathematical problem, closed by the specification of the initial distribution of the remodelling variable, according to the scheme presented in equations (66)–(69) and in Table 2.

Beyond the choice of the remodelling variable, the treatment of the external remodelling force features a relevant difference with respect to that done by Olsson and Klarbring [53], who expressed the external remodelling force  $Z_e$  (with the notation adopted here) as

$$Z_e := \frac{\partial \hat{W}}{\partial Q}(\Phi_f, \bar{\mathbf{C}}, Q_T), \quad (70)$$

where  $Q_T$  represents a *target angle*. Substituting (70) into (43) yields

$$\dot{Q} = \frac{1}{\Gamma} \left( \frac{\partial \hat{W}}{\partial Q}(\Phi_f, \bar{\mathbf{C}}, Q_T) - \frac{\partial \hat{W}}{\partial Q}(\Phi_f, \bar{\mathbf{C}}, Q) \right), \quad (71)$$

which means that the choice (70) of  $Z_e$  leads to a stop of fibre reorientation when  $Q$  reaches the target value  $Q_T$ . In our study, we do account for the external force  $Z_e$  in the presentation of the mathematical model, but we set it equal to zero in numerical simulations. Since this amounts to describing the case in which the interaction with the environment is either switched off or so weak that the contribution of external forces is fairly negligible, we are actually solving

$$\dot{Q} = \frac{1}{\Gamma} \left( - \frac{\partial \hat{W}}{\partial Q}(\Phi_f, \bar{\mathbf{C}}, Q) \right). \quad (72)$$

Still, looking at (48), which defines the right-hand-side of (72), and at its evolution over time (cf. Figure 4), we see that the force triggering structural reorganisation, i.e.,  $-\partial \hat{W} / \partial Q$ , tends towards zero as time progresses. Thus, granted the balance of internal forces, our system naturally tends towards a stationary value of  $Q$ , which depends only on deformation and volumetric fraction of the fibres. One might argue that the result (72) is closely related to the choice of  $\hat{W}$ , whereas using an appropriate  $Z_e$  (e.g., as in (70)) supplies a criterion that, independently on the choice of  $\hat{W}$ , determines the conditions under which remodelling ceases, i.e., when  $Q$  approaches one of all

the physically meaningful solutions of the stationary equation  $Z_e = \partial \hat{W} / \partial Q$ . However, if we rely on such a criterion, we must be always able to compute a physically sound  $Z_e$ .

Another concern addresses the hypotheses that the dissipation function is differentiable for all  $\Omega$ , and homogeneous of degree two in this variable. Although these hypotheses are usually dictated by computational simplicity, the resulting model may be too restrictive, for it leads to (42), meaning that  $\hat{Y}(\Lambda, \Omega)$  vanishes with vanishing  $\Omega$ , and that remodelling starts as soon as  $Y$  is different from zero. Perhaps, in some circumstances, a more realistic assumption could be to assume that remodelling starts when the dissipative force reaches a positive target value  $Y_0(\Lambda)$ , which plays the role of a yield “stress”. In this case, much inspiration can be taken from the theory of rate-independent plasticity [59]. By doing so, it can be shown that, if the mechanical behaviour of a material is independent on  $\Omega$ , neither  $\hat{W}$  nor  $\hat{\mathbf{S}}_d$  may depend on  $\Omega$  (cf., e.g., [8]), and the force  $\hat{Y}$  depends on the sign of  $\Omega$  rather than on  $\Omega$  itself. To this end, the dissipation can be specified constitutively as a homogeneous function of degree one, i.e.,  $\hat{D}(\Lambda, \Omega) = Y_0(\Lambda)|\Omega|$  (as in perfect rate-independent plasticity), with  $\hat{D}$  being smooth in  $\Lambda$ , continuous for all values of  $\Omega$ , but non-differentiable at  $\Omega = 0$ . Hence, applying (40b) in the regions of differentiability of  $\hat{D}$  leads to

$$Y = \hat{Y}(\Lambda, \text{Sign}(\Omega)) = \begin{cases} Y_0(\Lambda), & \text{if } \Omega > 0, \\ -Y_0(\Lambda), & \text{if } \Omega < 0, \end{cases} \quad (73)$$

and the reorientation of fibres, i.e.,  $\Omega \neq 0$ , occurs as long as the condition

$$y(Y, \Lambda) := |Y| - Y_0(\Lambda) = 0 \quad (74)$$

is satisfied. Since the sign of  $\Omega$  is the same as the sign of  $Y$ , one can write

$$\Omega = \kappa \frac{\partial y}{\partial Y} = \kappa \text{Sign}(Y), \quad Y \neq 0, \quad \kappa \geq 0, \quad (75)$$

together with the Karush-Kuhn-Tucker conditions  $\kappa \geq 0$ ,  $y(Y, \Lambda) \leq 0$ , and  $\kappa y(Y, \Lambda) = 0$ . The multiplier  $\kappa$  is then determined by means of the consistency condition  $\kappa \dot{y}(Y, \Lambda) = 0$ . Equation (74)

603 defines a “yield”-criterion, with  $y$  being the yield-function, and  $Y_0(\Lambda)$  being the target value of  $Y$   
604 that determines the onset of fibre re-orientation. If  $\Omega$  is zero, the dissipation vanishes identically,  
605  $Y$  belongs to the subdifferential of  $\hat{D}$  at  $\Omega = 0$ , i.e.,  $Y \in ]-Y_0(\Lambda), Y_0(\Lambda)[$  [55, 8], and  $y(Y, \Lambda) < 0$ .  
606 Using models of fibres reorientation inspired by formal analogies with the Theory of Plasticity is  
607 still part of our current investigations.

608 The main limitation of our model is that the functional form of the PDD is assumed to be  
609 known from the outset. Thus, given  $\wp$  at the instant of time  $t_0$ , the structural reorganisation of the  
610 material preserves the functional form of the original distribution throughout the whole remodelling  
611 process. This could be too restrictive for some applications. In order to solve this problem, we are  
612 currently investigating the feasibility of a model of structural reorganisation in which the PDD  
613 itself plays the role of the remodelling variable, and is determined by an appropriate balance law.

614 A natural generalisation of the results presented in this paper could be achieved by studying the  
615 reorientation of fibres in a growing medium, while considering the structural remodelling induced  
616 by growth. The resulting framework could be extended to a constitutive description involving the  
617 second gradient of deformation and/or the gradient of the tensor of inelastic distortions due to  
618 growth. Such a programme requires the formulation of constitutive models featuring higher-order  
619 tensors. To handle these, the tools and suggestions presented by Auffray et al. [1] and Ferretti et  
620 al. [24] should be considered and perhaps adequately further developed.

621 It should be remarked that second gradient theories have been recently proposed, for example,  
622 by Lekszycki and dell’Isola [41], Madeo et al. [43, 44] for different purposes. Synthesis and resorption  
623 phenomena in bone reconstructed with bio-resorbable material have been investigated by Lekszycki  
624 and dell’Isola [41]. The biomechanical interactions between living bone and a bio-resorbable graft  
625 after reconstructive surgery have been studied by Madeo et al. [43]. Finally, Madeo et al. [44], by  
626 means of Hamilton’s Principle of Stationary Action, deduced a set of equations for deformable,  
627 second gradient porous media partially saturated by compressible fluids. A relevant aspect of  
628 their results is that the evolution of the volumetric fractions of the fluids are neither prescribed  
629 constitutively (cf., for example, [50]) nor computed by solving balance laws in the sense of [64].  
630 Rather, the volumetric fractions are regarded as “Lagrangian parameters” of a suitably defined

631 Lagrangian density function and, as such, must satisfy the Euler-Lagrange equations obtained by  
 632 means of Hamilton's Principle.

633 In addition to growth, a careful thermodynamic study of tissue damage should be performed.  
 634 Studies in this direction have been recently done by Gasser [27] with application to abdominal  
 635 aneurysms, whereas some theoretical tools have been proposed by Cuomo and Contraffatto [11]  
 636 and Contraffatto and Cuomo [10] within the framework of Elastoplasticity and Damage. To tackle  
 637 biomechanical problems in which a tissue is viewed as a multi-phasic mixture featuring solids  
 638 and fluids, these concepts should be re-formulated in the context of Mixture Theory in order  
 639 to account for solid-fluid interactions and a treatment of the related dissipative effects. To this  
 640 end, it is perhaps interesting to remark that the dissipative dynamics of a system regulated by a  
 641 scalar quantity (such as  $Q$  in our work) satisfying an evolution equation of the type (43) could be  
 642 generalised as done by Carcaterra and Akay [7].

## 643 A Appendix. Fourth-order tensors

644 Let  $\mathbf{a} \in (T\mathcal{E} \otimes T\mathcal{E})_S$  and  $\mathbf{A} \in (T\mathcal{C} \otimes T\mathcal{C})_S$ . Then, the fourth-order tensors

$$\mathbb{I} := \frac{1}{2}(\mathbf{i} \underline{\otimes} \mathbf{i} + \mathbf{i} \overline{\otimes} \mathbf{i}), \quad \mathbb{I}^{ab}_{mn} = \frac{1}{2}(\delta^a_m \delta^b_n + \delta^a_n \delta^b_m), \quad (76)$$

$$\mathbb{I} := \frac{1}{2}(\mathbf{I} \underline{\otimes} \mathbf{I} + \mathbf{I} \overline{\otimes} \mathbf{I}), \quad \mathbb{I}^{AB}_{MN} = \frac{1}{2}(\delta^A_M \delta^B_N + \delta^A_N \delta^B_M) \quad (77)$$

645 define the identities in  $(T\mathcal{E} \otimes T\mathcal{E})_S$  and  $(T\mathcal{C} \otimes T\mathcal{C})_S$ , respectively. Indeed, it holds that  $\mathbb{I} : \mathbf{a} = \mathbf{a}$ ,  
 646 for all  $\mathbf{a} \in (T\mathcal{E} \otimes T\mathcal{E})_S$  and  $\mathbb{I} : \mathbf{A} = \mathbf{A}$ , for all  $\mathbf{A} \in (T\mathcal{C} \otimes T\mathcal{C})_S$ . The notation “:” means double-  
 647 contraction of indices, i.e.,  $[\mathbb{I} : \mathbf{a}]^{ab} = \mathbb{I}^{ab}_{mn} a^{mn}$  and  $[\mathbb{I} : \mathbf{A}]^{AB} = \mathbb{I}^{AB}_{MN} A^{MN}$ . The symbols  $\underline{\otimes}$  and  
 648  $\overline{\otimes}$  were introduced by Curnier et al. [12]. The tensors  $\mathbb{I}$  and  $\mathbb{I}$  admit the decompositions

$$\mathbb{I} = \mathbb{K} + \mathbb{M}, \quad \mathbb{K} := \frac{1}{3}(\mathbf{g}^{-1} \otimes \mathbf{g}), \quad \mathbb{M} := \mathbb{I} - \mathbb{K}, \quad (78)$$

$$\mathbb{I} = \mathbb{K} + \mathbb{M}, \quad \mathbb{K} := \frac{1}{3}(\mathbf{C}^{-1} \otimes \mathbf{C}), \quad \mathbb{M} := \mathbb{I} - \mathbb{K}. \quad (79)$$

649 Here,  $\mathbb{K}$  and  $\mathbb{M}$  extract, respectively, the volumetric and deviatoric parts of  $\mathbf{a}$  with respect to  $\mathbf{g}$ , i.e.,

$$\mathbf{a}_v = \mathbb{K} : \mathbf{a} = \frac{1}{3} \text{tr}[\mathbf{g}\mathbf{a}] \mathbf{g}^{-1}, \quad (80a)$$

$$\mathbf{a}_d = \mathbb{M} : \mathbf{a} = \mathbf{a} - \frac{1}{3} \text{tr}[\mathbf{g}\mathbf{a}] \mathbf{g}^{-1}, \quad (80b)$$

650 whereas  $\mathbb{K}$  and  $\mathbb{M}$  determine, respectively, the volumetric and deviatoric parts of  $\mathbf{A}$  with respect  
651 to the *pulled-back* metric induced by  $\mathbf{C}$  (which is the pull-back of  $\mathbf{g}$ ), i.e.,

$$\mathbf{A}_v = \mathbb{K} : \mathbf{A} = \frac{1}{3} \text{tr}(\mathbf{C}\mathbf{A}) \mathbf{B}, \quad (81a)$$

$$\mathbf{A}_d = \mathbb{M} : \mathbf{A} = \mathbf{A} - \frac{1}{3} \text{tr}(\mathbf{C}\mathbf{A}) \mathbf{B}. \quad (81b)$$

652 The tensors  $\mathbb{K}$  and  $\mathbb{M}$  are orthogonal, i.e.,  $\mathbb{K} : \mathbb{M} = \mathbb{M} : \mathbb{K} = \mathbf{0}$  ( $\mathbf{0}$  is the zero in the space of fourth-order  
653 tensors), and idempotent, i.e.,  $\mathbb{K} : \mathbb{K} = \mathbb{K}$  and  $\mathbb{M} : \mathbb{M} = \mathbb{M}$ . Analogous properties are satisfied by  $\mathbb{K}$   
654 and  $\mathbb{M}$ . The transposed tensors

$$\mathbb{I}^T := \frac{1}{2}(\mathbf{I}^T \underline{\otimes} \mathbf{I}^T + \mathbf{I}^T \overline{\otimes} \mathbf{I}^T), \quad \mathbb{K}^T := \frac{1}{3} \mathbf{C} \otimes \mathbf{B}, \quad (82a)$$

$$\mathbb{M}^T := \mathbb{I}^T - \mathbb{K}^T \quad (82b)$$

655 are applied on second-order tensors of the type  $\mathbf{Z} \in (T^*\mathcal{C} \otimes T^*\mathcal{C})_S$  and have properties analogous  
656 to those shown above. The notations  $\mathbb{K}$  and  $\mathbb{M}$  correspond to  $\mathbb{K}^*$  and  $\mathbb{M}^*$  introduced by Federico  
657 [18] in order to emphasise that these tensors are the pull-back of the spatial *true* volumetric (or  
658 spherical) and deviatoric operators  $\mathbb{K}$  and  $\mathbb{M}$ , respectively (cf. (80a) and (80b)).

## 659 Acknowledgments

660 The authors gratefully acknowledge the Goethe-Universität Frankfurt am Main (Frankfurt am  
661 Main, Germany), the German Ministry for Economy and Technology (BMW), contract 02E10326  
662 [A. Grillo and G. Wittum], the NSERC CREATE Programme (Natural Sciences and Engineering  
663 Research Council of Canada) [A. Tomic], the AITF New Faculty Programme (Alberta Innovates

– Technology Futures, formerly Alberta Ingenuity Fund, Canada) and the NSERC Discovery Programme (Natural Sciences and Engineering Research Council of Canada) [S. Federico].

## References

- [1] Auffray N, Bouchet R and Bréchet Y. Strain gradient elastic homogenisation of bidimensional cellular media. *International Journal of Solids and Structures* 2010; 47(13):1698–1710.
- [2] Aspden RM and Hukins DWL. Collagen organization in articular cartilage, determined by X-ray diffraction, and its relationship to tissue function. *Proc Roy Soc Lond Ser B* 1981; 212:299–304.
- [3] Ateshian GA. On the theory of reactive mixtures for modeling biological growth. *Biomechanical Model Mechanobiol* 2007; 6:423–445.
- [4] Barocas VH and Tranquillo RT. An anisotropic biphasic theory of tissue-equivalent mechanics: the interplay among cell traction, fibrillar network deformation, fibril alignment, and cell contact guidance. *J Biomech Eng* 1997; 119:137–145.
- [5] Bilby AB, Gardner LRT and Stroh AN. Continuous distributions of dislocations and the theory of plasticity. Proceedings of XI ICTAM (Brussels, 1957) Vol. III, Presses de l’Université de Bruxelles, 35–44, 1957.
- [6] Bonet J and Wood RD. Nonlinear Continuum Mechanics for Finite Element Analysis, Cambridge University Press, Cambridge New York, 2008.
- [7] Carcaterra A and Akay A. Dissipation in a finite-size bath. *Physical Review E* 2011; 84:011121-1–011121-4.
- [8] Cermelli P, Fried E and Sellers S. Configurational stress, yield and flow in rate-independent plasticity. *Proc R Soc A* 2001; 457:1447–1467.
- [9] Chadwick P. Continuum Mechanics, Concise Theory and Problems, Dover Publications Inc., Mineola, 1976.

- [10] Contrafatto L and Cuomo M. A new thermodynamically consistent continuum model for hardening plasticity coupled with damage. *International Journal of Solids and Structures* 2002; 39:6241–6271.
- [11] Cuomo M and Contrafatto L. Stress rate formulation for elastoplastic models with internal variables based on augmented Lagrangian regularisation. *International Journal of Solids and Structures* 2000; 37:3935–3964.
- [12] Curnier A, He QC and Zysset P. Conewise linear elastic materials. *J Elasticity* 1995; 37:1–38.
- [13] deBotton G and Shmuel G. Mechanics of composites with two families of finitely extensible fibers undergoing large deformations. *J Mech Phys Solids* 2009; 57:1165–1181.
- [14] DiCarlo A and Quiligotti S. Growth and Balance. *Mech Res Commun* 2002; 29:449–456.
- [15] Driessen NJB, Peters GWM, Huyghe JM, Bouten CVC and Baaijens FPT. Remodelling of continuously distributed collagen fibres in soft connective tissues. *J Biomech* 2003; 36(8):1151–1158.
- [16] Epstein M and Maugin GA. Thermodynamics of volumetric growth in uniform bodies. *Int J Plasticity* 2000; 16:951–978.
- [17] Eringen AC. *Mechanics of Continua*, Krieger, Melbourne, FL, 1980.
- [18] Federico S. Covariant formulation of the tensor algebra of non-linear elasticity. *Int J Nonlinear Mech* 2012; 47(2):273–284.
- [19] Federico S and Herzog W. On the permeability of fibre-reinforced porous materials. *Int J Solids Struct* 2008; 45(7–9):2160–2172.
- [20] Federico S and Herzog W. On the anisotropy and inhomogeneity of permeability of articular cartilage. *Biomechan Model Mechanobiol* 2008; 7(5):367–378.
- [21] Federico S and Grillo A. Non-linear elasticity and permeability of fibre-reinforced porous media. *Mech Mater* 2012; 44:58–71.



- [22] Federico S, Grillo A and Herzog W. A transversely isotropic composite with a statistical distribution of spheroidal inclusions. *J Mech Phys Solids* 2004; 52:2209–2327.
- [23] Federico S, Grillo A, La Rosa G, Giaquinta G and Herzog W. A transversely isotropic, transversely homogeneous statistical model of articular cartilage. *J Biomech* 2005; 32:2008–2018.
- [24] Ferretti M, Madeo A, dell’Isola F, Boisse P. Modeling the onset of shear boundary layers in fibrous composite reinforcements by second gradient theory. *Zeitschrift für angewandte Mathematik und Physik ZAMP* 2013; DOI 10.1007/s00033-013-0347-8.
- [25] Flory PJ. Thermodynamic relations for high elastic materials. *Trans Faraday Soc* 1961; 41:829–838.
- [26] Fung YC. Biomechanics: Motion, Flow, Stress, and Growth, Springer-Verlag Inc., New York, 1990.
- [27] Gasser TC. An irreversible constitutive model for fibrous soft biological tissue: A 3-D microfiber approach with demonstrative application to abdominal aortic aneurysms. *Acta Biomater* 2011; 7:2457–2466.
- [28] Gasser TC, Gallinetti S, Xing X, Forsell C, Swedenborg J and Roy J. Spatial orientation of collagen fibers in the abdominal aortic aneurysm’s wall and its relation to wall mechanics. *Acta Biomater* 2012; 8:3091–3103.
- [29] Gasser TC, Ogden RW and Holzapfel GA. Hyperelastic modelling of arterial layers with distributed collagen fibre orientations. *J Roy Soc Interface* 2006; 3:15–35.
- [30] Glansdorff P and Prigogine I. Thermodynamic theory of structure, stability and fluctuations. Wiley-Interscience, London, 1971.
- [31] Grillo A, Federico S and Wittum G. Growth, mass transfer and remodeling in fiber-reinforced, multi-constituent materials. *Int J Nonlinear Mech* 2012; 47:388–401.
- [32] Grillo A, Federico S, Wittum G, Giaquinta G, Imatani S and Mićunović MV. Evolution of a fibre-reinforced mixture. *Nuovo Cimento C* 2009; 32(1):97–119.

- [33] Gurtin ME. Generalized Ginzburg-Landau and Cahn-Hilliard equations based on a microforce balance. *Physica D* 1996; 92:178–192.
- [34] Hackl K and Fischer FD. On the relation between the principle of maximum dissipation and inelastic evolution given by dissipation potentials. *Proc R Soc A* 2008; 464:117–132.
- [35] Holzapfel GA, Gasser TC and Ogden RW. A new constitutive framework for arterial wall mechanics and a comparative study of material models. *J Elasticity* 2000; 61:1–48.
- [36] Hughes TJR. The Finite Element Method – Linear Static and Dynamic Finite Element Analysis. Dover Publications, Inc. Mineola, New York, 2000.
- [37] Imatani S and Maugin GA. A constitutive model for material growth and its application to three-dimensional finite element analysis. *Mech Res Commun* 2002; 29:477–483.
- [38] Kröner E. Die inneren Spannungen und der Inkompatibilitätstensor in der Elastizitätstheorie. *Z Angew Math Phys* 1959; 7:249–257.
- [39] Kroon M. A continuum mechanics framework and a constitutive model for remodelling of collagen gels and collagenous tissues. *J Mech Phys Solids* 2010; 58:918–933.
- [40] Lee EH. Elastic-plastic deformation at finite strains. *ASME Transaction on Journal of Applied Mechanics* 1969; 36:1–6.
- [41] Lekszycki T and dell’Isola F. A mixture model with evolving mass densities for describing synthesis and resorption phenomena in bones reconstructed with bio-resorbable materials. *ZAMM Z. Angew. Math. Mech* 2012; 92(6):426–444.
- [42] Loret B and Simões FMF. A framework for deformation, generalized diffusion, mass transfer and growth in multi-species multi-phase biological tissues. *European Journal of Mechanics A/Solids* 2005; 24:757–781.
- [43] Madeo A, Lekszycki T and dell’Isola F. A continuum model for the biomechanical interactions between living tissue and bio-resorbable graft after bone reconstructive surgery. *Comptes Rendus Mecanique* 2011; 339:625–640.

- [44] Madeo A, dell’Isola F and Darve F. A continuum model for deformable, second gradient porous media partially saturated with compressible fluids. *Journal of the Mechanics and Physics of Solids* 2013; 61(11):2196–2211.
- [45] Marsden JE and Hughes TJR. Mathematical Foundations of Elasticity, Dover Publications Inc., New York, 1983.
- [46] Menzel A. Modelling of anisotropic growth in biological tissues. *Biomech. Model Mechanobiol.* 2005; 3:147–171.
- [47] Menzel A. A fibre reorientation model for orthotropic multiplicative growth. Configurational driving stresses, kinematics-based reorientation and algorithmic aspects. *Biomech Model Mechanobiol* 2007; 6(5):303–320.
- [48] Mollenhauer J, Aurich M, Muehleman C, Khelashvili G, Irving TC. X-Ray Diffraction of the Molecular Substructure of Human Articular Cartilage. *Conn Tiss Res* 2003; 44:201–207.
- [49] Mow VC and Guo XE. Mechano-Electrochemical Properties of Articular Cartilage: Their Inhomogeneities and Anisotropies. *Annu Rev Biomed Eng* 2002; 4:175–209.
- [50] Nedjar B. Formulation of a nonlinear porosity law for fully saturated porous media at finite strains. *Journal of the Mechanics and Physics of Solids* 2013; 61:537–556.
- [51] Ogden RW. Nearly isochoric deformations: Application to rubberlike solids. *J Mech Phys Solids* 1978; 26:37–57.
- [52] Ohsumi TK, Flaherty JE, Evans MC, and Barocas VH. Three-dimensional simulation of anisotropic cell-driven collagen gel compaction. *Biomechan Model Mechanobiol* 2008; 7:53–62.
- [53] Olsson T and Klarbring A. Residual stresses in soft tissue as a consequence of growth and remodelling: application to an arterial geometry. *Eur J Mech A/Solids* 2008; 27:959–974.
- [54] Rajagopal KR and Srinivasa AR. On thermomechanical restrictions of continua. *Proc R Soc A* 2004; 460:631–651.

- 785 [55] Rockafellar RT. Convex Analysis, Princeton University Press, New Jersey, 1970.
- 786 [56] Rodriguez EK, Hoger A, McCullogh AD. Stress-dependent finite growth in soft elastic tissues.  
787 *J Biomech* 1994; 27:455–467.
- 788 [57] Salsa S. Partial Differential Equations in Action — From Modelling to Theory, Springer-  
789 Verlag, Milan Heidelberg New York, 2008.
- 790 [58] Schriefl AJ, Zeindlinger G, Pierce DM, Regitnig P and Holzapfel GA. Determination of the  
791 layer-specific distributed collagen fibre orientations in human thoracic and abdominal aortas and  
792 common iliac arteries. *J R Soc Interface* 2012; 9:1275–1286.
- 793 [59] Simo JC and Hughes TJR. Computational Inelasticity, Springer, New York Heidelberg, 1998.
- 794 [60] Taber LA. Biomechanics of growth, remodeling and morphogenesis. *ASME Appl Mech Rev*  
795 1995; 48:487–545.
- 796 [61] Truesdell C and Noll W. The Non-Linear Theories of Mechanics, 3rd Edition, Springer-Verlag  
797 Berlin Heidelberg, 1965.
- 798 [62] Tsamis A, Krawiec JT and Vorp DA. Elastic and collagen fibre microstructure  
799 of the human aorta in ageing and disease: a review. *J R Soc Interface* 2013;  
800 <http://dx.doi.org/10.1098/rsif.2012.1004>.
- 801 [63] Walpole LJ. Elastic behavior of composite materials: theoretical foundations. *Adv Appl Mech*  
802 1981; 21:169–242.
- 803 [64] Wilmanski K. On Thermodynamics of Nonlinear Poroelastic Materials. *Journal of Elasticity*  
804 2003; 71:247–261.